Paleowind Direction and the Regional Pattern of Grain Size and Atterberg Limits of Loess in Adams and Lincoln Counties, WA

Charlie Chou

A report prepared in partial fulfillment of
the requirements for the degree of

Masters of Science
Earth and Space Science: Applied Geosciences
University of Washington
January 2020

Reading Committee:
Kathy Troost
Steven Walters

Reviewers: Crystal Lambert

Message Technical Report Number:085

Abstract

Loess is a fine-grained floury material carried by wind. The properties of loess are important for infrastructure, agriculture, and construction planning in areas where it is abundant. Eastern Washington is one such location where loess hills dominate the landscape. Past studies have established the geologic origins of loess in Eastern Washington on a broad regional scale. These studies established that paleowinds carried the loess Northeast and that gran size decreases downwind. Naturally, I set out to ask if the paleowind direction and subsequent decrease in grain size can be detected over a smaller two county area. To answer this, I collected 27 samples of loess in Adams and Lincoln counties to determine its index properties and look for regional patterns in grain size. I analyzed grain size, moisture content, and Atterberg limits. Then I evaluated the results in a geographic information system. I found that paleowind influence can be found in the grain size and properties of the loess within Adams and Lincoln counties. The results of my study provide insight into the general characteristics of loess index properties in parts of Eastern Washington and confirm the results from previous work.

Table of Contents

List of Figures

Acknowledgements

I wish to express my sincere appreciation to Dr. Kathy Troost who guided, challenged, and encouraged me throughout this project. She also provided facilities, equipment, and planning help necessary to complete my analysis. Without her help, this project would not have been possible. I also wish to acknowledge the support of my classmates in Cohort 7, especially Crystal Lambert, for giving me honest feedback and support while working on this project.

1. Introduction

Eastern Washington, east of the Cascade Mountains, is drier in climate than the western portion of Washington and includes Adams and Lincoln counties, the focal area of this

study. Abundant deposits of fine, floury windborne material called loess dominate the upland surficial deposits in these counties. This loess formed from a rich Quaternary history in the Pacific Northwest that links multiple geologic processes (Sweeney et al., 2017; McDonald and Busacca, 1992; McDonald and Busacca, 2012). Between 13,000 to 15,000 years ago, the Missoula Floods, part of a series of glacial outburst floods, carved through hills into the bedrock of Eastern Washington, forming coulees and depositing large amounts of sediment for paleowinds to later transport back east across the region as loess. This pattern of extensive water-driven deposition followed by redistribution by paleowinds has been repeated at least 3 times in the Quaternary (McDonald et al. 2012). The direction of the paleowind was deciphered from variations in the loess over the large scale of Eastern Washington but can paleowind be inferred over small areas? Does grain size decrease downwind in the loess within Adams and Lincoln Counties? Such a trend would provide support pointing to the paelowind direction as a driving factor in transport and deposition. To address this I collected 27 samples of the loess from across the 2-county area to geographically compare grain sizes and Atterberg limits. Studying the patterns of loess is insightful for both local and regional road planning as well as construction (Eske, 1959) because, when building on loess, the physical in-situ strength of loess changes based on moisture levels, grain size, and plasticity. The strength and behavior of loess is important because it affects infiltration, agriculture, and infrastructure. Grain size and Atterberg limits are direct controls on the strength and behavior of loess.

2. Background

2.1 Location

The physiography of southeastern Washington consists mainly of rolling hills and plains with private lands primarily purposed for agriculture. The study area is south of Spokane, north of Walla Walla, and east of the Columbia River (Figure 1A). Samples were taken in Washtucna, Ritzville, Lind, Providence, Janz, Odessa, Mohler, Harrington, and Davenport. The area receives on average 11 to 14 inches of rain per year and has a predominant wind direction in the East to Northeast. The loess is notably beneficial for growing agriculture.

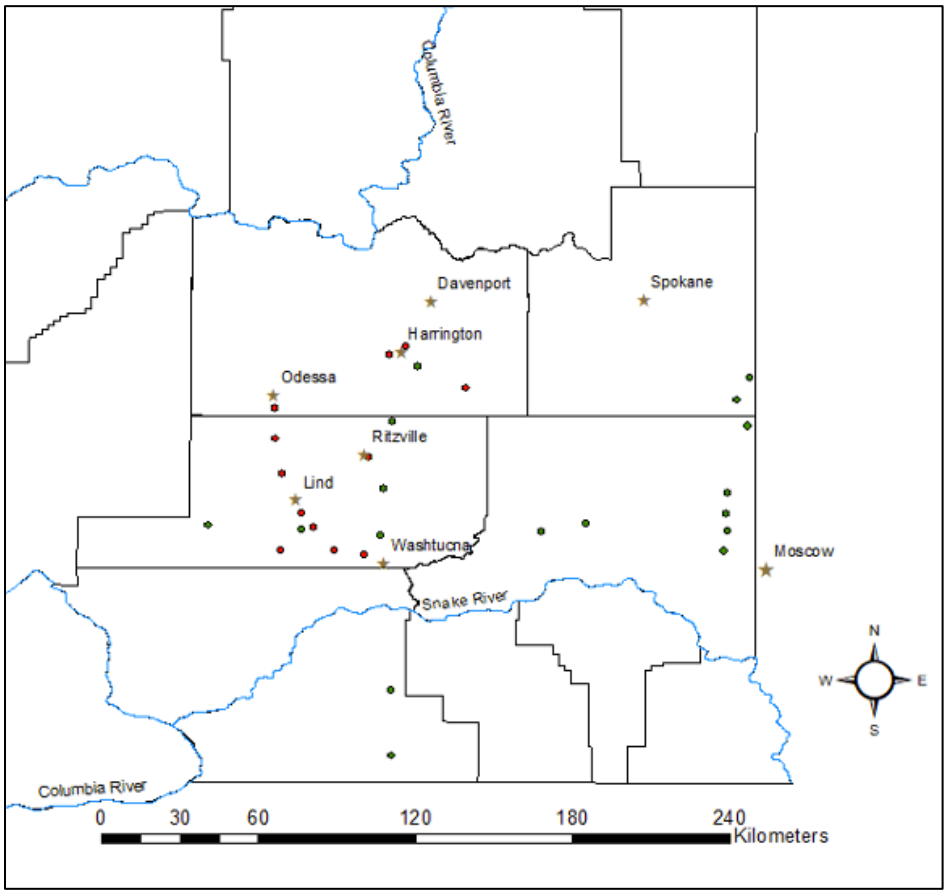

Figure 1A. Location map with cities and rivers labeled. Samples marked as dots.

2.2 Geology

Following the end of the last glacial maximum, several episodes of glacial outburst floods roared over the landscape of Eastern Washington, carving deep troughs and depositing vast amounts of sediment into the south-central reaches of the Columbia Basin (Figure 1). Paleowinds then carried this sediment back to the Northeast forming the rolling hills mantled with loess of present day. Eske (1959) initially categorized the loess deposits into three pedogenic groups – Ritzville, Walla Walla, and Palouse – despite the engineering properties of each being similar. Therefore Eske's (1959) boundaries were not used for my studies. I placed Eske's groups into one group, Eastern Washington loess.

According to Gaylord et al. (2003), loess covers more than 50,000 km^2 with deposits that are from a few meters to 75 m thick. Clay, silt, and sandy facies are present in the loess. Sand dunes southwest of my study area cover from 20 km^2 at the Sand Hills Coulee to more than 1000 km^2 in the Quincy dunes in the area. Eastern Washington loess rests on the Miocene Columbia River Basalt at elevations ranging from 200 m along the eastern margin of the Pasco Basin in Washington to approximately 800 m near Moscow, Idaho (Gaylord et al., 2003).

Several times in the Quaternary, glaciation led to ice damming and failure of the dams led to outburst floods which scoured into basalt to create coulees. At Wallua gap, damming led to water ponding. Sediment deposited in these ponds and were dispersed once the ponds disappeared by wind to the Northeast. Sand was deposited near the source, silt was deposited at medium distance, and clay was deposited at distal far away areas.There was

continued reworking during interglacial periods and today sand dunes are migrating in this area to the East.

Foley (1982) gives general descriptions of the loess in four roadcuts near Washtucna. McDonald and Busacca, 1992 also discuss six roadcuts in the Cheney-Palouse Scabland Tract of the Channeled Scabland of Washington to the south of Foley's sites.

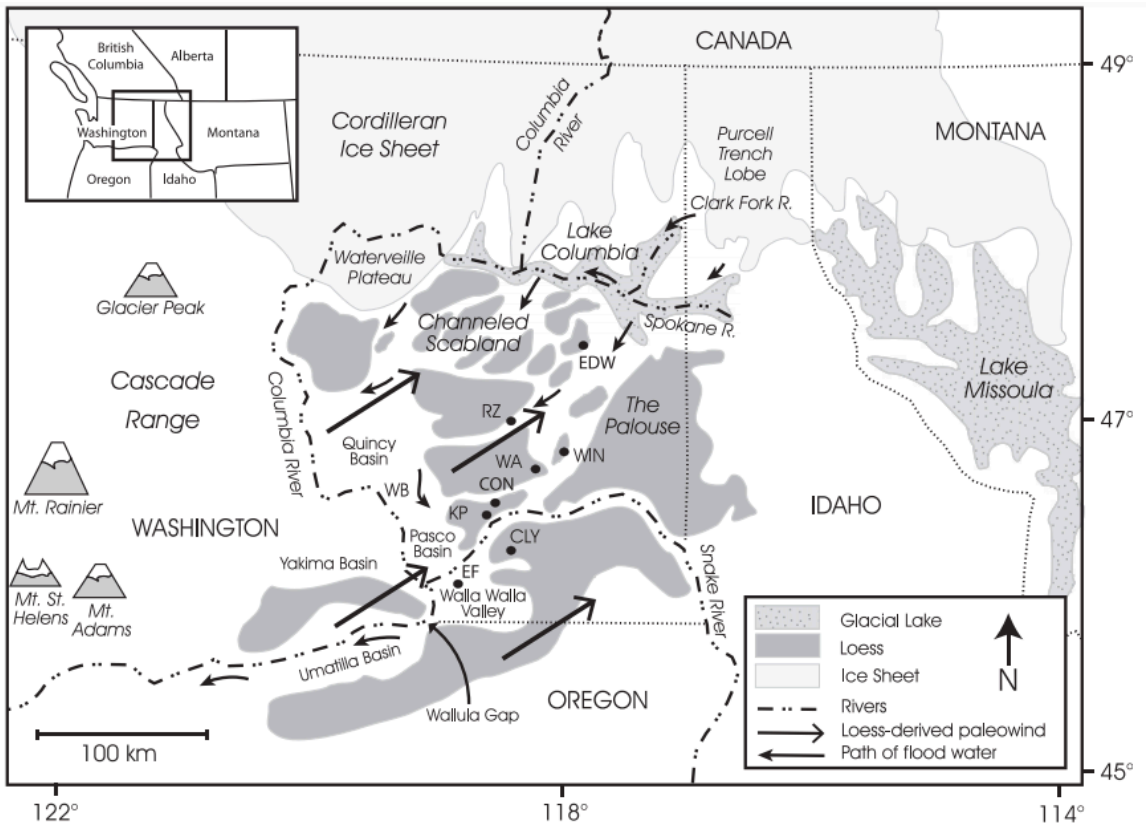

Figure 1B. Map of Pacific Northwest showing the loess deposits and surrounding area as a proxy record of ice sheet advances and related glacial outburst floods after the last glacial maximum. Paleowind direction is in large arrows and path of flood water during the Missoula floods is in smaller arrows. Sites from Mconald et al. (2012) are abbreviated EF for Eureka Flat, WA for Washtucna, RZ for Ritzville, WB for White Bluffs, EDW for Edwall, WIN for Winona, CON for Connell, and KP for Kennewick. (Modified from McDonald et al., 2012.)

McDonald and Busacca (1992) describe the loess as consisting of fine sand- and silt-sized quartz, feldspar, and mica with minor amounts of heavy minerals and volcanic glass. They mention the loess is weakly calcareous with 2 to 8 wt% detrital carbonate. The loess also contains paleosols that represent periods of calm. By comparison, paleosols in the area have cylindrical nodules of calcite or silica.

2.3 Loess L1 and L2

Researchers have also described the basic stratigraphic sequence and features of Eastern Washington loess layers, the overlying paleosols, tephra layers, and flood-cut unconformities in the loess record (McDonald and Busacca, 1994). This regional stratigraphic framework suggests the most recent layers of loess are connected to the two most recent episodes of Channeled Scabland flooding. McDonald et al. (2012) describe these as the L1 and L2 loess layers (Figure 2). Using luminescence dating, they suggest the L1 loess was deposited after the outburst flood from glacial Lake Missoula during the late Wisconsin glaciation while the L2 layer was deposited after the outburst flooding between 74 and 58 ka after the OIS 4 glaciation. I focused my study on the L1 loess layer.

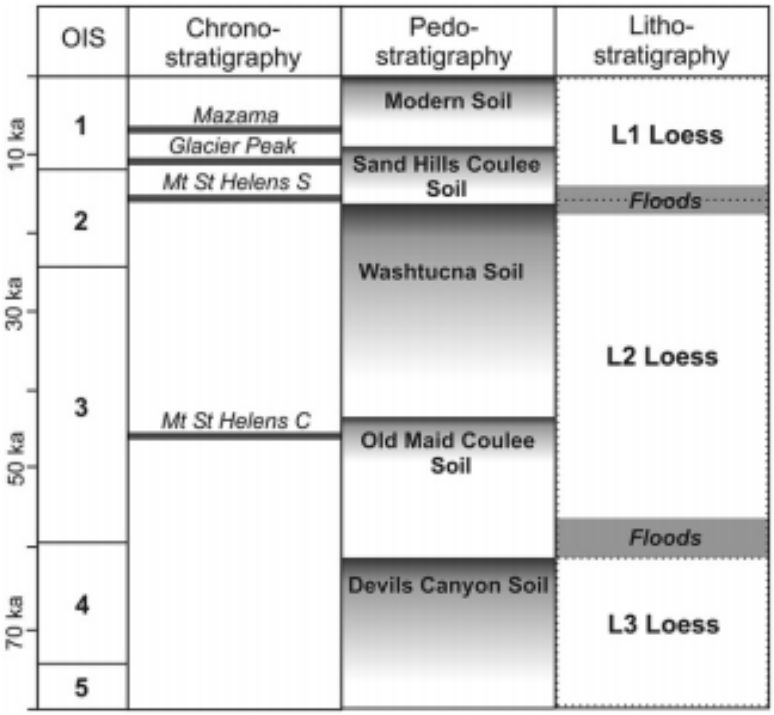

Figure 2. Regional stratigraphy used in McDonald et al. (2012) including chronostratigraphic (ash layer) markers. Oxygen Isotope Stage (OIS) is used to correlate with time.

The L1 loess is capped by modern surface soil and contains Mount St. Helen's S tephra at its base, which is reported to be around 15.5 to 15.8 ka (McDonald et al., 2012). Regional trends in thickness of L1 loess decreases northeast and downwind. L1 loess thickness is estimated at around 450 centimeters at Sand Hills Coulee (McDonald et al., 2012). Loess accumulations are generally thickest closest to source material area. This is because a significant portion of suspension load transported by wind is coarse silt and very fine sand that can only be moved short distances. Fine silt and clay can be mobilized much farther by the wind. McDonald et al., (2012) and Ludwig (1987) speculated that Eastern Washington loess transported by paleowind would follow the same pattern.

2.4 Previous Work on Grain Size

Higgins et al. (1985) in a study for the Washington Department of Transportation (WSDOT), looked at strength parameters to design drainage schemes for protecting road cut slopes from erosion. Higgins et al. (1985) tested loess from different depth intervals and at different locations in the Pacific Northwest (Figure 6). Using sieve and hydrometer analyses, Higgins et al. (1985) classified loess as sandy, silty, or clayey based on grain size distribution (Figure 3). Higgins also compared plasticity data for the Eastern Washington loess as a way to classify the loess (Figure 4). They found that the fine grained component of the loess ranges from low plasticity silt (ML) to low plasticity clay (CL). The distribution of grain size and plasticity from samples allow comparisons between loess across different regions of the United States and prediction of engineering behavior. Higgins et al. (1985) also found that, in general, the grain size decreases and the plasticity increases with increasing distance from Eureka Flat in the east direction.

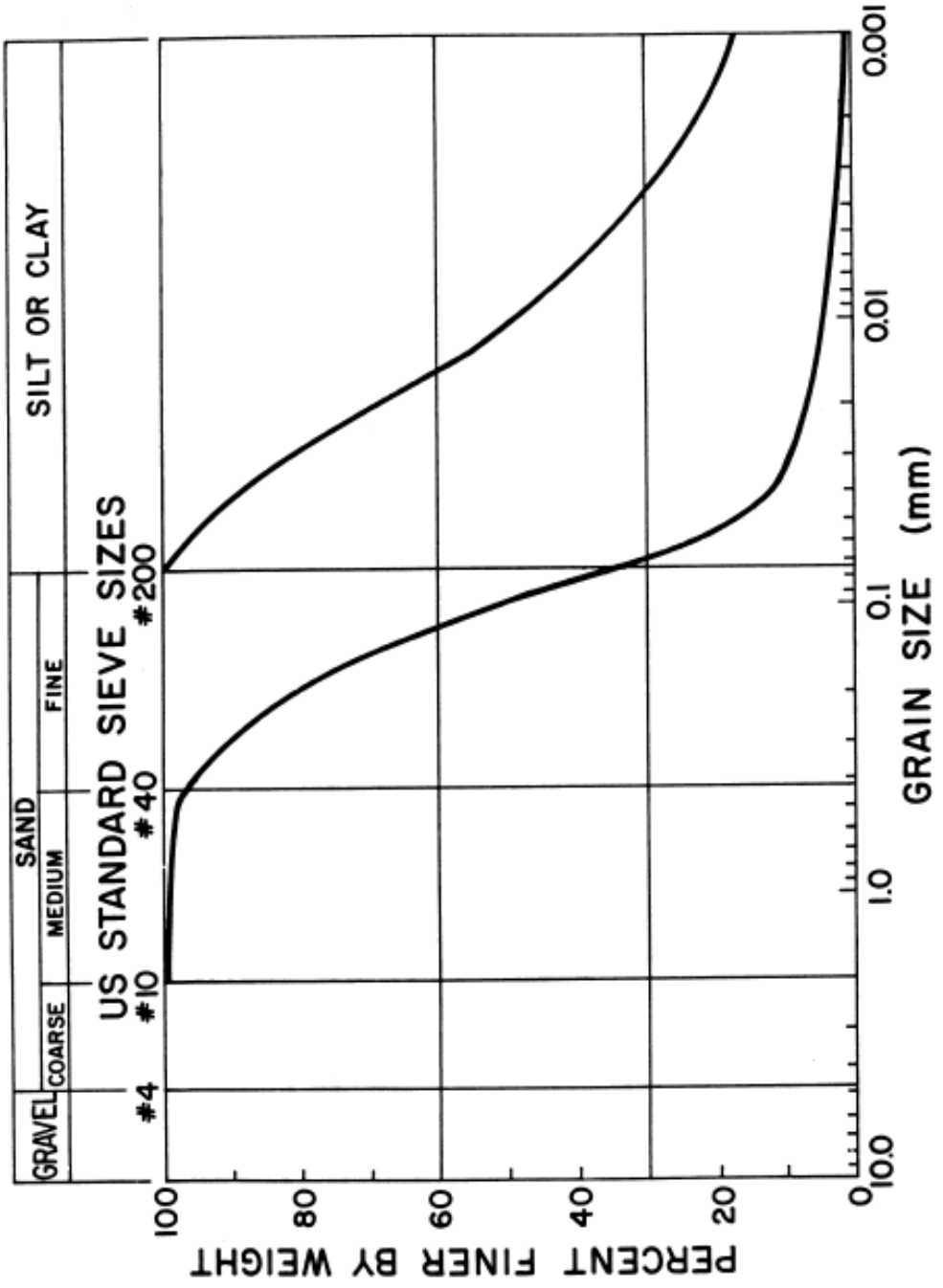

Figure 3. Range in grain size distribution of samples of Southeastern Washington loess (modified from Higgins et al., 1985). Grain size ranges from silty, fine sand, to clayey silt, to silty clay to fine sandy silt.

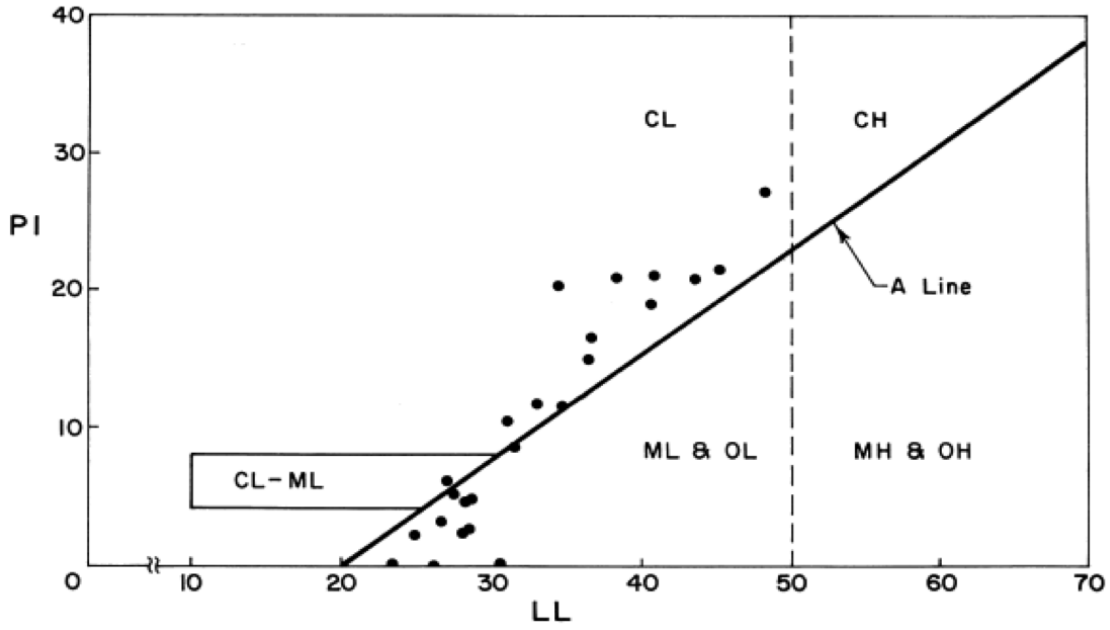

Figure 4. Plasticity data for southeastern Washington loess in Washington Department of Transportation study (modified from Higgins et al., 1985). PI is plasticity index, LL is liquid limit, ML is low plasticity silt, MH is high plasticity silt, OL is low plasticity organics, OH is high plasticity organic silt, CL is low plasticity organic silt, CH is high plasticity clay.

3 Methods

To determine if I could detect a paleowind influence in Adams and Lincoln county loess, I collected samples and looked for regional patterns in my samples moving from east to west, north to south, and southwest to the northeast. I determined Atterberg Limits and grain size distributions as the basis for my comparisons.

3.1 Sample Collection

To conduct an analysis on the Eastern Washington loess, I designed an initial sampling plan by selecting sites across Adams and Lincoln Counties using Landsat aerial photography from Google Earth. This area was chosen because it provided a large distribution of loess in a broadly northeastern direction. The goal was to evenly space my sampling sites along a northeast transect. However, my collection sites were limited

to accessible roadcuts on road easements. I used a shovel to sample below the modern soil horizon in the loess deposits at accessible roadcuts. Sample sites ultimately selected based on outcrop quality and access.

After scraping off loose weathered material, fresh loess samples were collected at twenty seven locations (Figure 5) and stored in quart-sized Ziploc bags. At each collection site, I recorded time, date, road cut height, slope aspect, depth of sample, identifying features unique to each site, and the latitude and longitude coordinates from Avenza and Google Maps in WGS 1984 geographic earth-fixed terrestrial reference system (Table 1). I assumed that sampling from the upper layers of the Loess would allow me to sample in the L1 layer previously described by McDonald et al. (2012). I dug around 0.6 to 1 meter below ground surface before sampling. In order to ensure a representative sample, I avoided sampling in streams, valleys, and rivers, due to possible disturbance or erosion of loess in these settings.

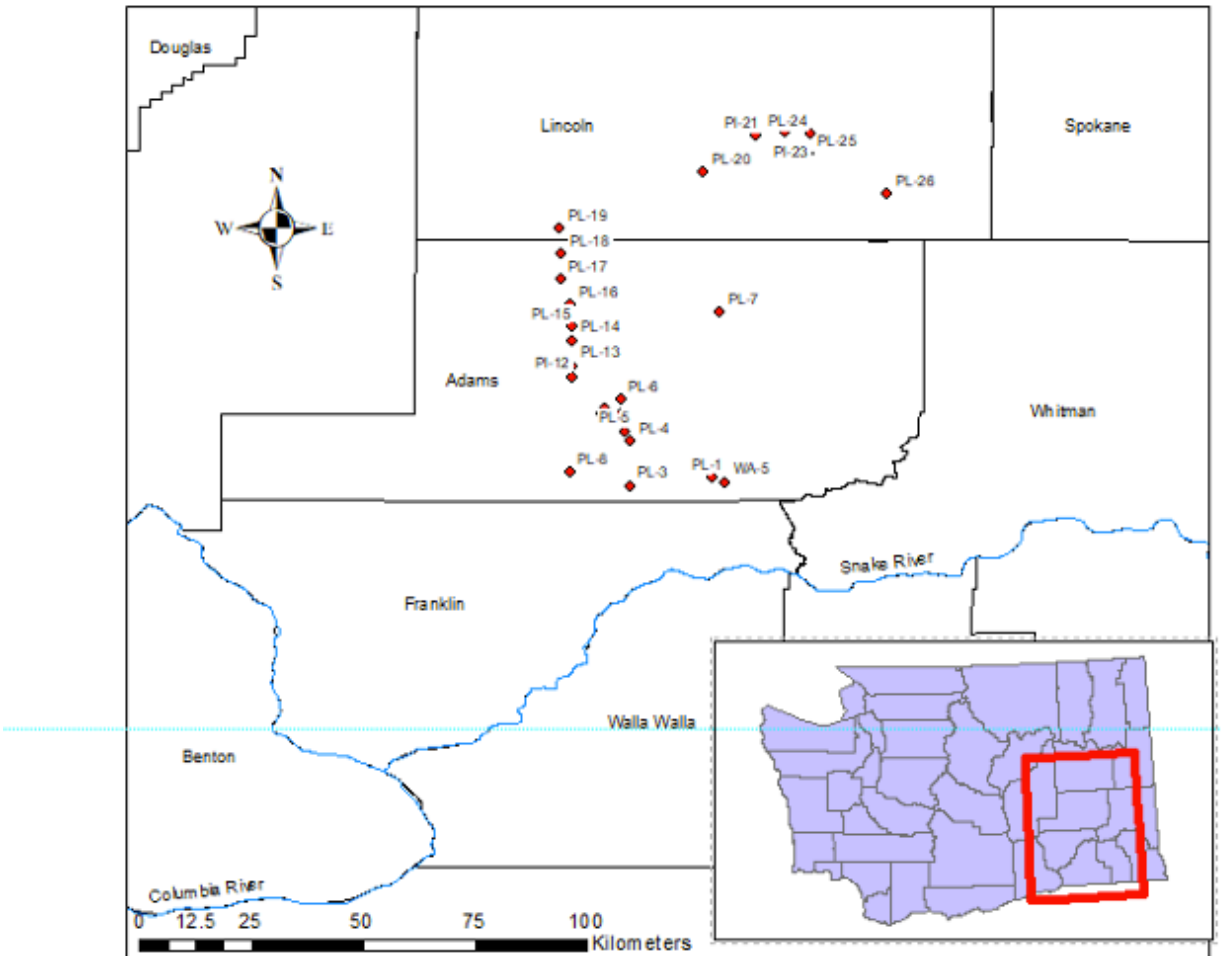

Figure 5A. Map of my sample locations relative to Eastern Washington. The intersection of the Columbia River with the Snake River where Franklin, Benton, and Walla Walla counties come together can be used to orient to Figure 1, Figure 5A, and Figure 5B.

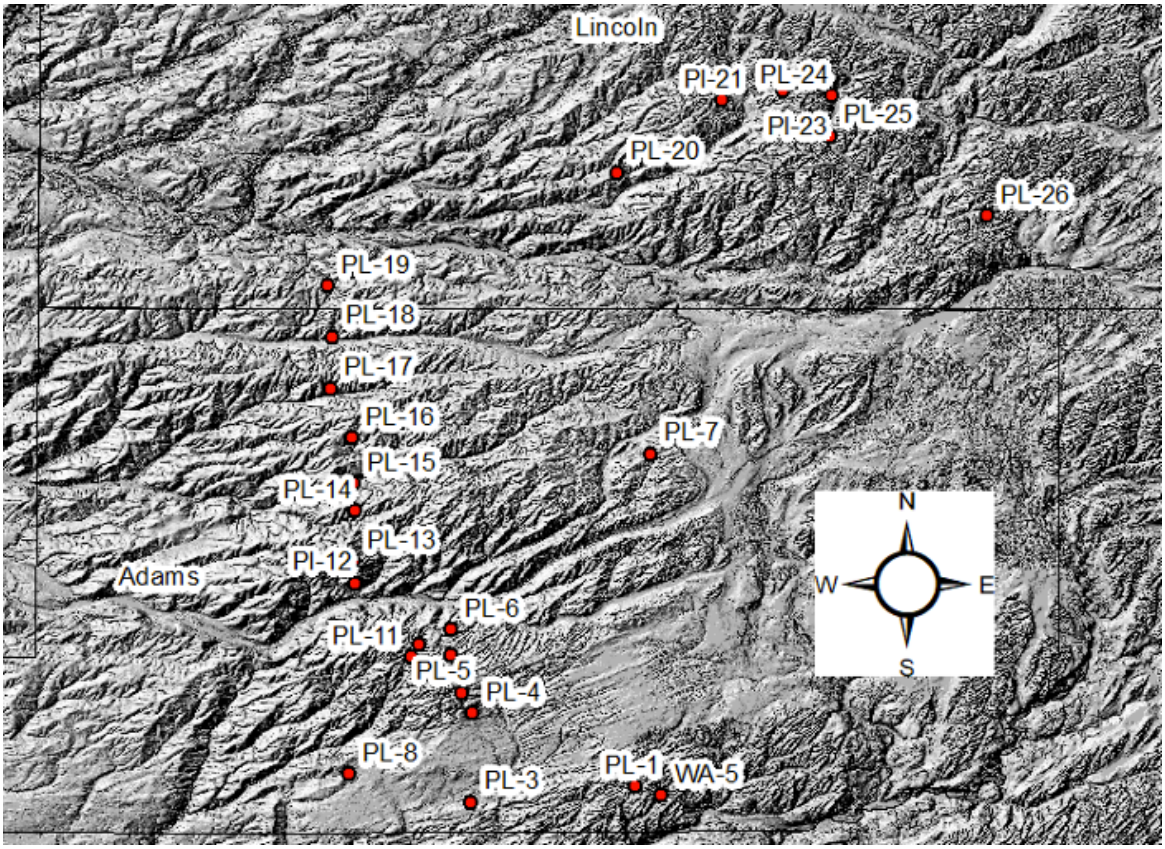

Figure 5B. Zoom on sites of previous site map with lidar for sample locations in Southeastern Washington loess.

Table 1. Summary of Sampling Field Notes

Sample ID	Location	Roadcut height (meters)	Slope Aspect	Taken From	Notes
PL-1	46.78213,-118.38234	7.6	N	Middle L2	CaCO3 cement. At Mile Marker 79
WA-5	46.77302, -118.35729	5.5	SW	Upper outcrop	Previous WA-5 site from McDonald and Busacca
PL-2	46,79551,-118.48545	4	SW	0.61 m BGS	No roadcut, side of road next to farm
PL-3	46.76639, -118.54741	0.9	E	0.61 m BGS	Near farm with Dunes
PL-4	46.85576,-118.54651	0.9	W	0.61m BGS	Mole Burrows present in roadcut
PL-5	46.87603, -118.55698	6.1	SW	0.61m BGS	6.1`m unvegetated deposit, spiders
PL-6	46.93886, -118.56718	2.4	E	0.9-1.22m BGS	Mile Marker 22, Roadcut hill
PL-7	47.11471,-118.36777	-0.9	N	0.9-1.22m BGS	Loves Travel Station Excavation

PL-8	46.79459,-118.66916	5.5	S	0.9 m Below top of roadcut	
PL-1B	46.78213,-118.38234	7.6	N	1.52m Below top of roadcut,	Resampled for L1
PL-9	46.91275,-118.56722	1.5	W	0.61m Below top	Intersection: Providence Rd and St HWY 21 NW intersection corner.
PL-10	46.92356,-118.59875	4.3	E	1.22m below top	Along HWY395 Southbound
PL-11	46.91208,-118.60618	4.3	W	0.61m below top of roadcut	Along HWY395 Northbound
PL-12	46.98549,-118.66359	0.9	E	0.61m below top	Near utility warning pole
PL-13	47.00735,-118.66398	4	E	0.61-0.9m below top	Columnar to Massive Deposit
PL-14	47.05788,-118.66309	0.9	E	0.61m below top	Mole burrows present in roadcut
PL-15	47.08498,-118.66487	4.9	W	0.9m below top of roadcut	Sampled from loess above basalt
PL-16	47.13079,-118.66617	1.8	S	0.9m below top	
PL-17	47.18042,-118.68773	2.7	W	0.61m below top	
PL-18	47.23207,-118.68628	4	W	0.61m below top	
PL-19	47.28342,-118.69036	0.9	W	0.61m below top	Road next to Farm
PL-20	47.39642,-118.40166	0.6	SW	0.61m, Ground level	
PL-21	47.46847,-118.29591	2.7	NW	0.61m below top	
PL-22	47.49628,-118.24080	4.4	NW	0.9m below top of roadcut	
PL-23	47.47821,-118.23574	3.7	N	0.9m below top of roadcut	
PL-24	47.47380,-118.18725	6.4	E	0.9m below top	
PL-25	47.43324,-118.18835	1.5	W	0.61m below top	
PL-26	47.35345,-118.03142	1.2	S	0.61m below top	

3.2 Laboratory Testing

a) Grain Size

I used sieve analysis to assess particle size distributions of the loess samples. I selected twelve samples to wash, dry, and run through a series of stacked sieves from larger to smaller mesh (#4, #10, #20, #40, #100, and #200) (Table 2). After sieving using a mechanical sieve shaker, the percent passing was recorded for each sample. From the data, I classified the loess based on the percent passing in each sieve. The sieve analyses were done in accordance with ASTM C136 and completed in the Earth and Space Science Engineering Geology laboratory at University of Washington.

Table 2. Sieze size used

Sieve #	Diam (mm)
4	4.75
10	2
20	0.84
40	0.42
100	0.15
200	0.075
<200	0.002

b) Moisture Content

I found the moisture content for an aliquot of each sample following ASTM D-2216. This involved first determining a wet weight, then drying the sample in an oven at 110 degrees Celsius, then measuring the dry weight to determine the weight of water loss.

c) Atterberg Limits

The samples were tested using ASTM D423-66 (Liquid Limit) and D424-59 (Plastic Limit) to attain Atterberg Limits. The Atterberg limits measure the critical water contents of the loess to estimate its shrinkage limit, plastic limit, and liquid limit. The value of

these limits allow one to identify the loess's soil classification and use empirical correlations to determine engineering properties such as compressibility, permeability, and strength. Samples were prepared by adding water to break apart clumps and by using a #40 screen to remove CaCO3 nodules and medium sand.

Liquid Limits were determined using a Casagrande device. Samples were mixed into a uniform paste of soil and water and spread into the Casagrande cup. A groove was cut through the center of the paste using a standard grooving tool. The cup was dropped 10mm at a rate of 2 drops per second until the two sides of the groove flowed together and made contact across a distance of about 10 mm. The number of blows required to close the groove was recorded and the procedure was repeated twice more. The water content for the material in the closed groove was determined so that the water content vs. 25 blows could be discerned.

The Plastic Limit of a soil is the water content at the boundary between plastic and semi-solid states. The soil paste is rolled into 3.175mm diameter threads and rerolled until the thread cracks or crumbles at 3.175mm in diameter. The water content is then determined on the crumbled or cracked threads.

d) Classification/Description

Soil colors were found using a Munsell color chart. I classified the samples using ASTM D-2487 and 2488 and the Unified Soil Classification System. My descriptions include features noted in the field like the presence of CaCO3 and gravel.

3.3 Digitization/Office Work

Once soil properties were accurately measured I visualized changes in the loess over distances. I used ArcMap to spatially visualize the percent fines and Atterberg Limits. I

also added WGS1984 geographical location data from my sample site locations. I added lab data as attribute information for my points.

I also digitized sample locations from maps provided in Higgins et al. (1985) (Figure 6) to add more data for a better spatial picture. Georeferencing the points from county boundaries and river locations. I included data from related graphs in their paper as a way to link attribute data to each point. The Higgins et al. (1985) data provided percent weight verses distance graphs that I converted into percent passing values. Combining both my lab data with Higgins et al, (1985) data into one format, I made best fit transects from southwest to northeast following the inferred wind direction, from east to west like in Higgins' assessment, and north to south (Figure 9A). This allowed me to select the farthest samples on each end of a transect as end points and project the rest of the points into a clear ordered transect. I then divided the main transect into segments between each sample point to get distances between points (Figure 9D, 9E, 9F). I used ArcMap to calculate approximate length of segments in meters. With distances between points and attribute data for each point, I was able to graph changes in the loess over transect distances.

For elevations, I obtained 10-meter resolution digital elevation models (DEMs) from the USGS and hosted through the University of Washington's Earth and Space Science GIS webpage. I used the Mosaic to New Raster tool in ArcGIS to merge the raster outputs into a single DEM raster.

I also matched the coordinate system using Projection and Project Raster to UTM Zone 11N, NAD 1927. I used Search Tool and then add surface information to add Elevation to my attribute table for samples in my transects.

With a hillshade I was able to discern whether my transect points were in a valley, flatland, hillslope, or floodplain.

To visualize the terrain, I created a hillshade from my DEMs and I also color coded slope based on slope angle values.

With the sample sites, DEMs, and other derivatives I was able to classify each site based on geomorphology for appropriate use in my transects. Points in valley bottoms and floodplains were ignored because the loess in these areas was probably disturbed.

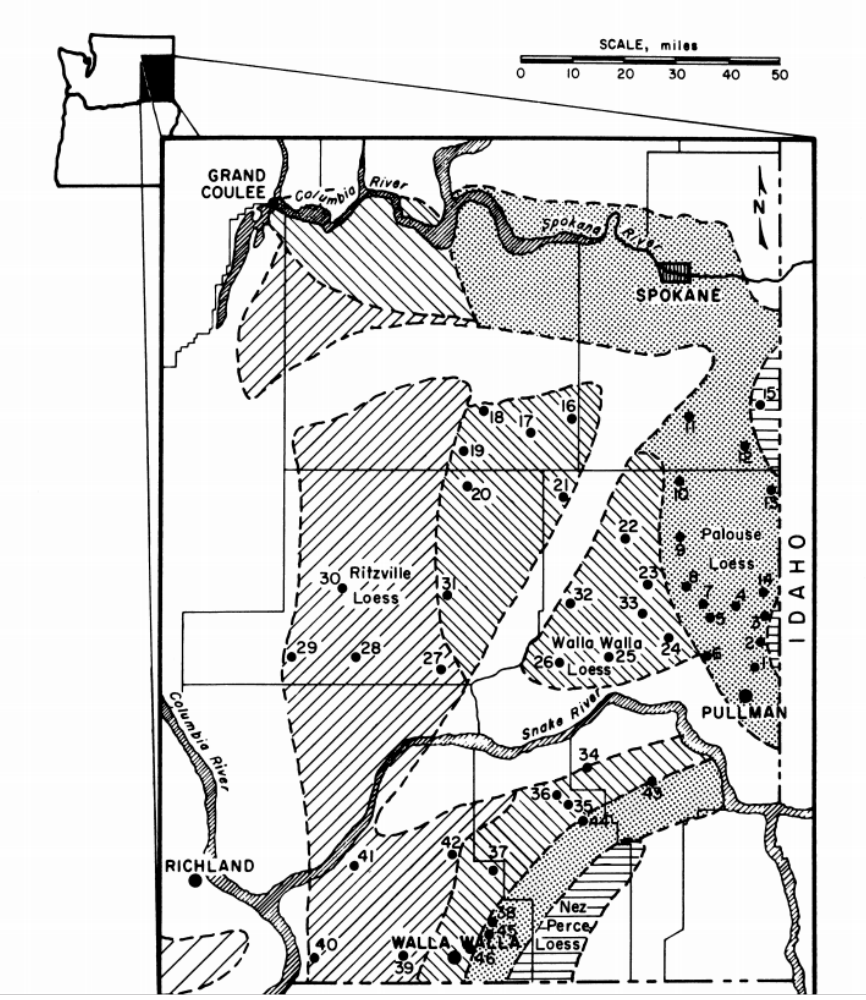

Figure 6. Sample locations for southeastern Washington loess in previous Washington Department of Transportation study (modified from Higgins et al. 1985).

4. Findings

4.1 Grain Size

I did a sieve analysis on twelve of my twenty-seven samples. These samples were selected because they represent a wide geographic distribution within my study area. I used the sieve data to create grain size distribution curves for samples: PL-1B, PL-2, PL-5, PL-7, Pl-8, PL-10, PL-14, PL-17, Pl-19, Pl-21, PL-22, and PL-26 (Figures 7A to 7L). The finer clay section of the curve from 0.1 to 0.001mm was not found because of inaccessibility to a hydrometer or lazer particle size analyzer. I used hydrometer results from close by samples from Higgins et al., (1985) to infer these sections when available.

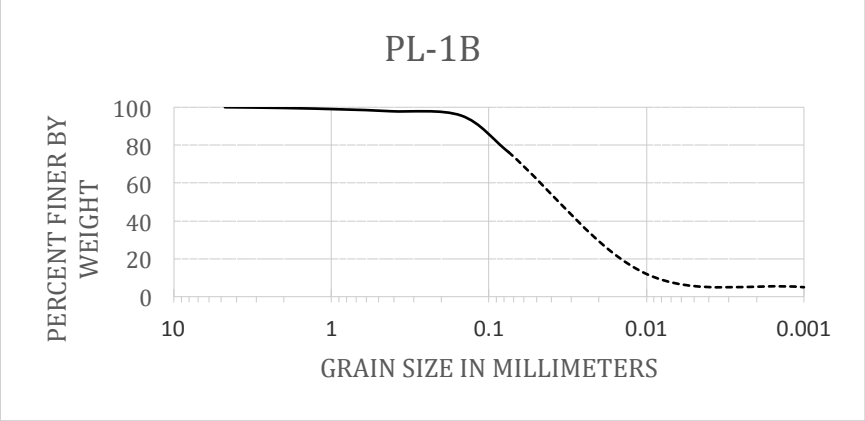

Figure 7A. Grain size distribution curve for sample PL-1B. Dashed line inferred from sample B-27 Higgins et al., (1985)

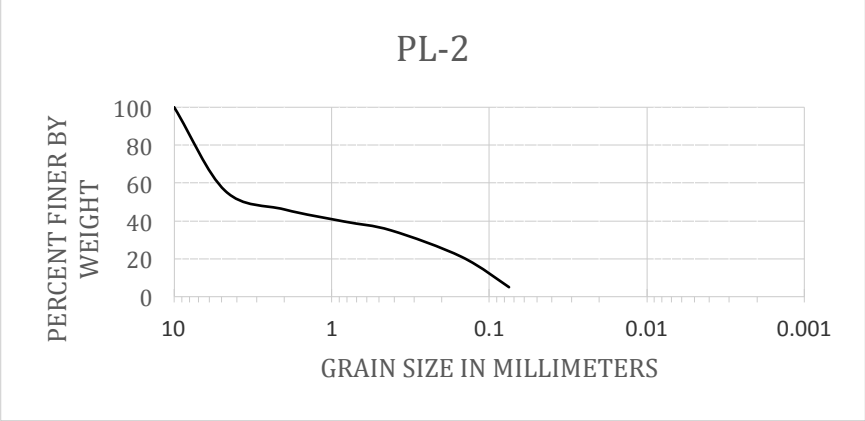

Figure 7B. Grain size distribution curve for sample PL-2.

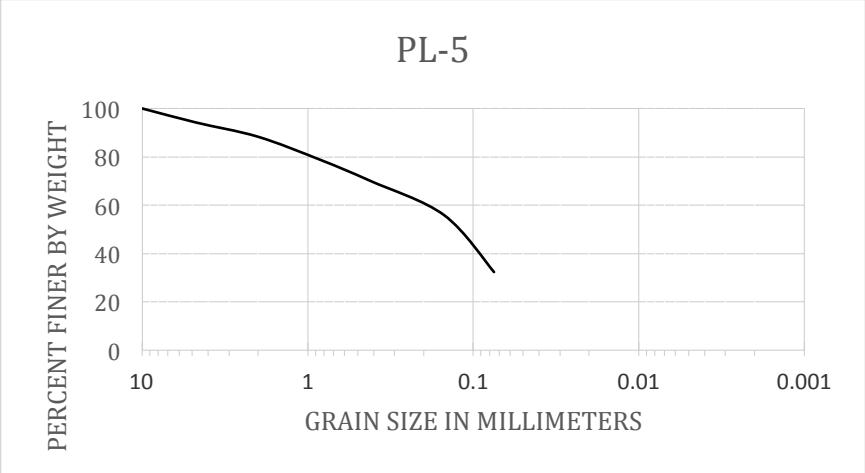

Figure 7C. Grain size distribution curve for sample PL-5.

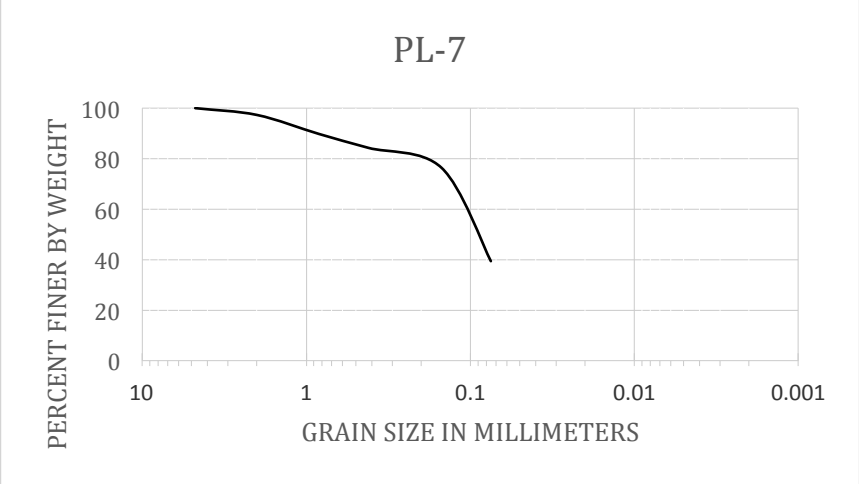

Figure 7D. Grain size distribution curve for sample PL-7.

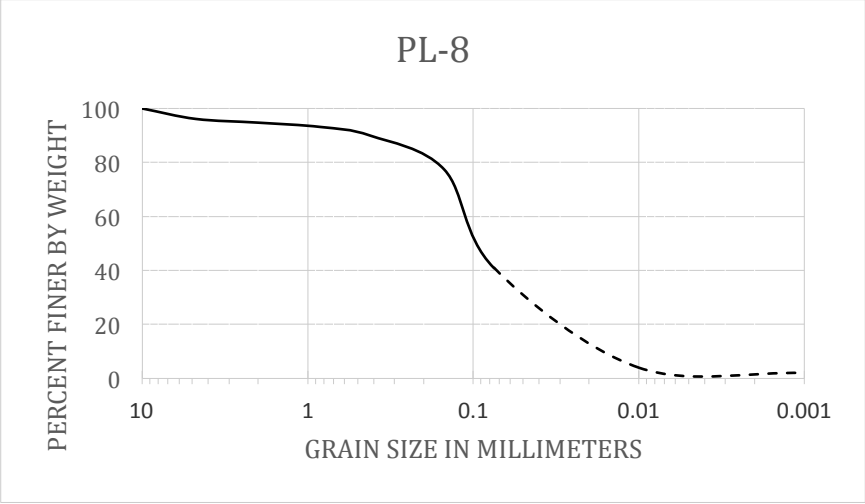

Figure 7E. Grain size distribution curve for sample PL-8. Dashed line inferred from sample B-28 in Higgins et al., (1985).

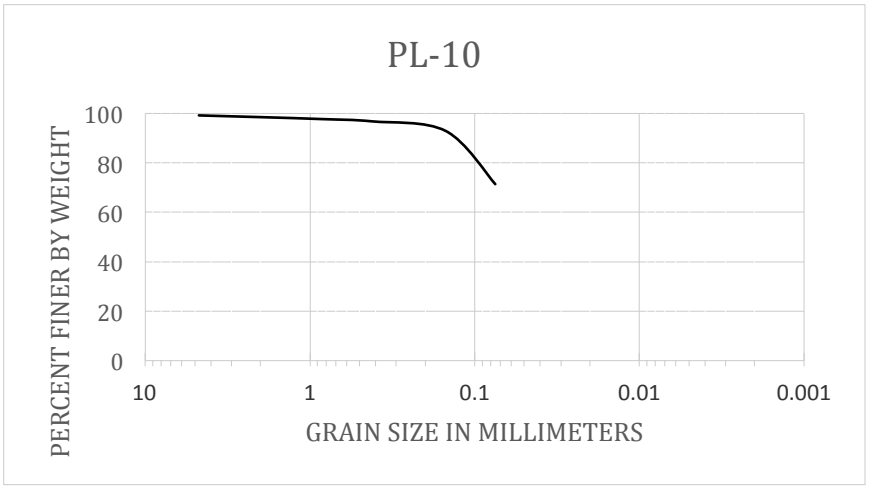

Figure 7F. Grain size distribution curve for sample PL-10.

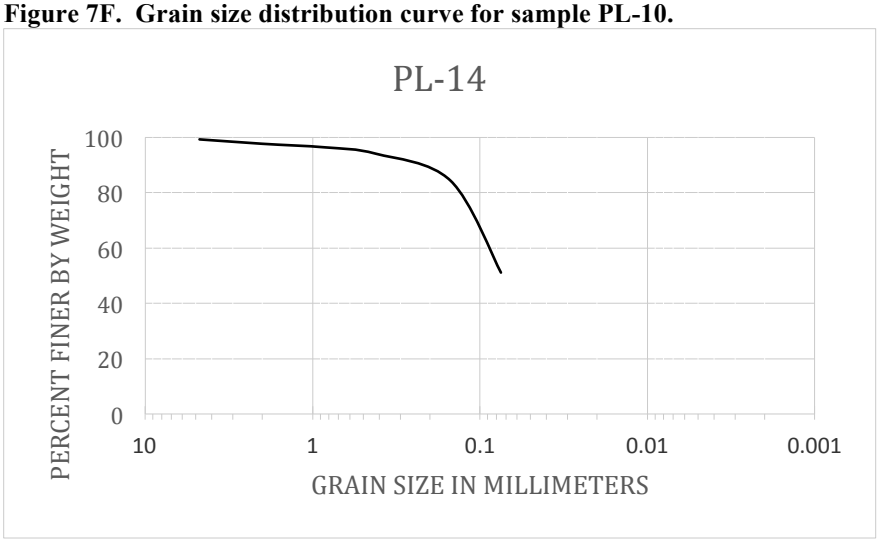

Figure 7G. Grain size distribution curve for sample PL-14.

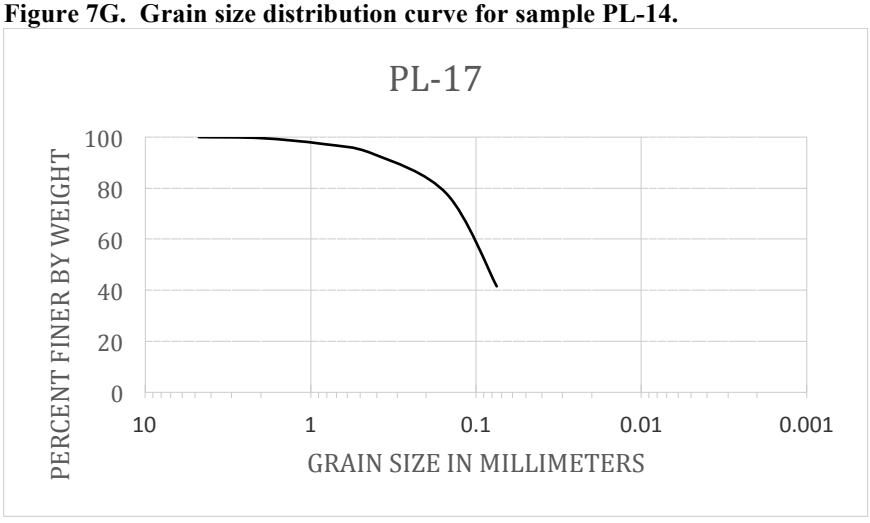

Figure 7H. Grain size distribution curve for sample PL-17.

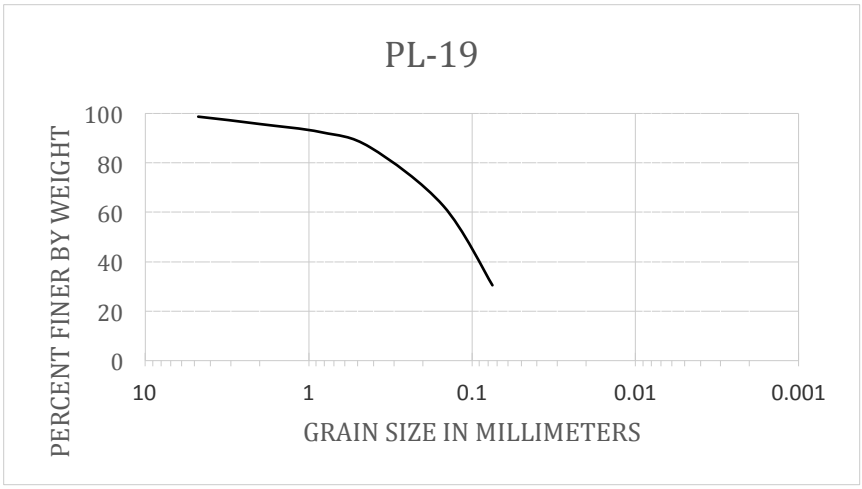

Figure 7I. Grain size distributions curve for sample PL-19.

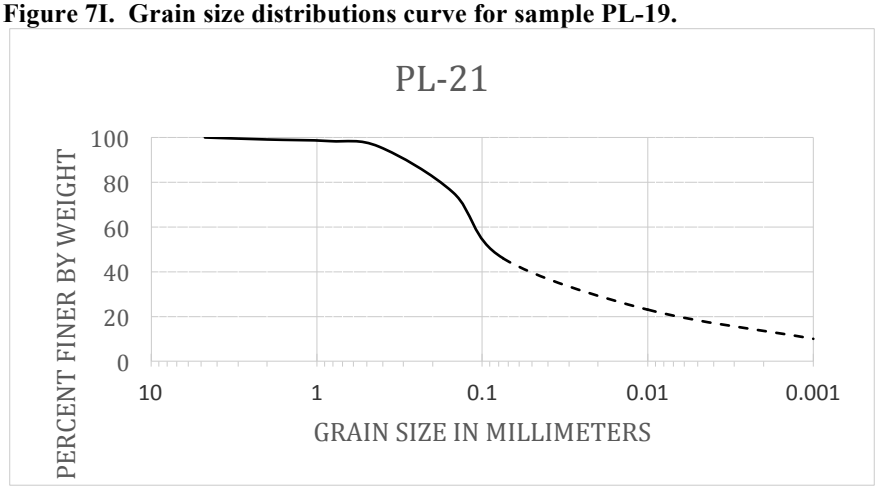

Figure 7J. Grain size distributions curve for sample PL-21. Dashed line inferred from sample B-18 in Higgins et al., (1985).

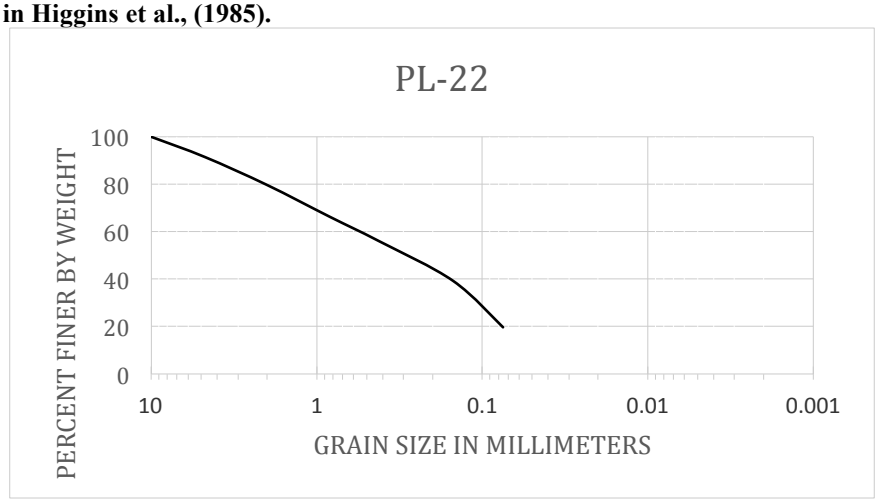

Figure 7K. Grain size distribution curve for sample PL-22.

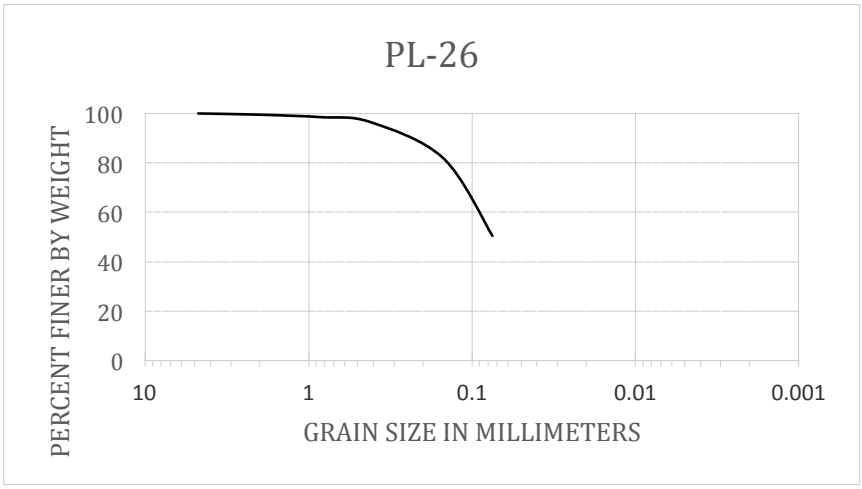

Figure 7L. Grain size distributions curve for sample PL-26.

I found that the samples I tested had variable grain size ranges. The grain size of the sieved samples ranged from fine gravelly coarse sand with trace silt at PL-2 to fine sandy silt at PL-1B to fine sandy, silty, clay at PL-5. The gravel sized particles generally consisted of CaCO3 nodules, but some transported gravel clasts were also seen. The percent fines (%finer than 0.075mm in diameter) in the samples tested ranged from 22% to 90% (Table 3).

4.2 Atterberg Limits

I determined Atterberg Limit values on all of my 27 samples. Based on Atterberg Limit testing done in the laboratory, I determined that the fines in my loess samples collected were mainly low plasticity silts (ML) with some low plasticity clays (CL) (Figure 8) (Table 3). My data complements data results found by Higgins et al. (1985) (Figure 4). Notably, my samples contained significantly fewer clays than Higgins et al. (1985), which I hypothesize is due to the distribution of my sampling locales not extending as far east as those collected in the other study. This explanation is supported by my distance to percent passing graphs (Figure 10A, Figure 10B, Figure 10C) which show a correlation that as one moves northeast and east, the percent passing of the local loess

generally increases. In other words, higher percent passing samples from the WSDOT study (1985) correlate with samples collected farther to the east. Conversely, based on the WSDOT data, clay percentage in the samples is higher to the North and East directions and lower in the opposite directions. This trend weakly correlates with Liquid Limit graphs made from the University of Washington sample data. Some of the fines in my loess samples were found to have no plasticity (PL-2, PL-6, Pl-7, PL-8, PL-10, PL-13, PL-16, PL-18, PL-20) and of these PL-2 and PL-8 were found to be sand. Since hydrometer analyses were not completed to estimate the percent clay partial size, the Atterberg Limit Values tell us if the fines are considered a clay or clayey (Table 3).

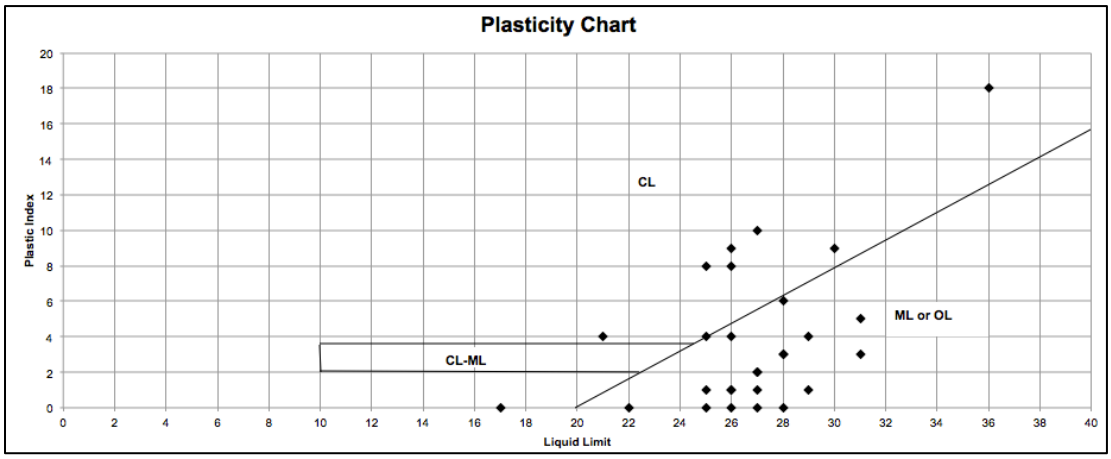

Figure 8. Plastic Index vs Liquid Limit of the soils collected for study.

4.3 Classification

Most of the loess samples had colors on the Munsell Color 2.5Y page transitioning from Pale Yellow in the southwest of the study area to Olive Yellow and Olive Brown in the northeastern reach of the sampling areas . This differs from the findings of McDonald and Busacca (1992) who classified most of their samples in the 10YR page of the Munsell Color chart. Using ASTM D2487, my loess samples were mainly silts with low plasticity

or silty to very fine sands with low plasticity and a few of samples were inorganic clays of low plasticity.

Table 3. Summary Loess Sample Description and Classifications

Sample ID	Munsell Color (in lab)	Soil Description	Geomorphology	Fines %	LL,PI	USCS
PL-1	2.5Y 7/4 Pale Yellow	loose, low plasticity silt	Valley Slope	**87**	**28,3**	**ML**
WA-5	2.5Y 7/4 Pale Yellow	loose sand with low plasticity silt	Valley Slope	**-**	**25,0**	**SM**
PL-2	10YR 8/2 White	loose, low plasticity silty clay	Flat	**22**	**17,0**	**SC**
PL-3	2.5Y 6/2 Light Brownish Gray	loose, low plasticity silty clay	Flat	**-**	**21,4**	**CL**
PL-4	2.5Y 6/6 Olive Yellow	loose, low plasticity, silty clay	Valley Slope	**-**	**28,6**	**CL**
PL-5	2.5Y 6/6 Olive Yellow	loose, fine sand with low plasaticity clay	Gully Slope	**64**	**25,8**	**CL**
PL-6	2.5Y 6/6 Olive Yellow	loose, low plasticity, silt	Gully Slope	**-**	**26,0**	**ML**
PL-7	2.5Y 6/6 Olive Yellow	loose, low plasticity, silt	Valley Slope	**90**	**22,0**	**ML**
PL-8	2.5Y 7/6 Yellow	loose, fine sand with low plasticity silt	Flat	**81**	**26,1**	**ML**
PL-1B	2.5Y 7/4 Pale Yellow	loose, low plasticity silt	Valley Slope	**87**	**28.5,3.5**	**ML**
PL-9	2.5Y 5/4 Light Olive Brown	loose, low plasticity silt	Gulley Slope	**-**	**27,2**	**ML**
PL-10	2.5Y 6/6 Olive Yellow	loose, low plasticity, silt	Gully Slope	**83**	**26,1**	**ML**
PL-11	2.5Y 5/4 Light Olive Brown	loose, low plasticity silt	Gully Slope	**-**	**26.5,1.5**	**ML**
PL-12	2.5Y 6/6 Olive Yellow	loose, low plasticity, silty clay	Valley Slope	**-**	**25,3**	**CL**

PL-13	2.5Y 7/6 Yellow	loose, low plasticity silt	Gully Slope	-	29,1	ML
PL-14	2.5Y 6/6 Olive Yellow	loose, low plasticity silt	Gully Slope	86	26,4	ML
PL-15	2.5Y 7/6 Yellow	loose, low plasticity silty clay	Valley Slope	-	26,9	CL
PL-16	2.5Y 7/6 Yellow	loose, low plasticity silt	Gully Slope	-	25,0	ML
PL-17	2.5Y 5/4 Light Olive Brown	loose, low plasticity silty clay	Gully Slope	93	27,10	CL
PL-18	2.5Y 6/6 Olive Yellow	loose, low plasticity silt	Valley Slope	-	25,1	ML
PL-19	2.5Y 5/4 Light Olive Brown	loose, low plasticity silty clay	Gully Slope	68	25.5,7.5	CL
PL-20	2.5Y 5/4 Light Olive Brown	loose, low plasticity silt	Gully Slope	-	28,0	ML
PL-21	2.5Y 5/4 Light Olive Brown	loose, low plasticity silt	Gully Slope	75	28,3	ML
PL-22	2.5Y 5/4 Light Olive Brown	loose, low plasticity, silty clay	Valley Slope	47	35.5, 17.5	SC
PL-23	2.5Y 5/4 Light Olive Brown	loose, fine sand with low plasticity silt	Gully Slope	-	30,9	SM
PL-24	2.5Y 5/4 Light Olive Brown	loose, low plasticity silty clay	Valley Slope	-	31,3	CL
PL-25	2.5Y 4/4 Olive Brown	loose, low plasticity silt	Valley Slope	-	26.5,0.5	ML
PL-26	2.5Y 4/4 Olive Brown	loose, low plasticity silt	Gully Slope	76	31,5	ML

4.4 Downwind Comparisons

Three transects and lab data are used to look for geographic patterns (Figure 9A). My data are supplemented with data from Higgins et al. (1985). Overall, the fines content of all the loess samples tends to decrease to the northwest along transect Z-Z'(Figure 10A) consistent with a decrease in the paelowind direction inferred by McDonald et al. (2012). However my samples show no strong trends. Overall the fines content of the loess samples tend to decrease from west to east along transect X-X' as well (Figure 10B). While the trend in my samples is stronger than northwest, it also does not show a strong correlation from west to east either. Overall, the fines content does not decrease from north to south along transect Y-Y' (Figure 10C). A source of difficulty could be from the data being too distal in the transects. The trend in plasticity with distance from the source area appears to be stronger than the trend in fines content.

From the maps, I confirmed that fine sand and silt settled faster than clays downwind. The percent passing generally increases as one moves downwind and larger grains disappear. The fines and clay percentage slightly increases downwind. This plays a role in Atterberg Limits at a local scale by slightly increasing the Liquid Limit downwind. Another approach to visualize downwind trends beyond linear transects involved contouring. I created contour lines of percent passing in intervals of ten percent (Figure 9C).

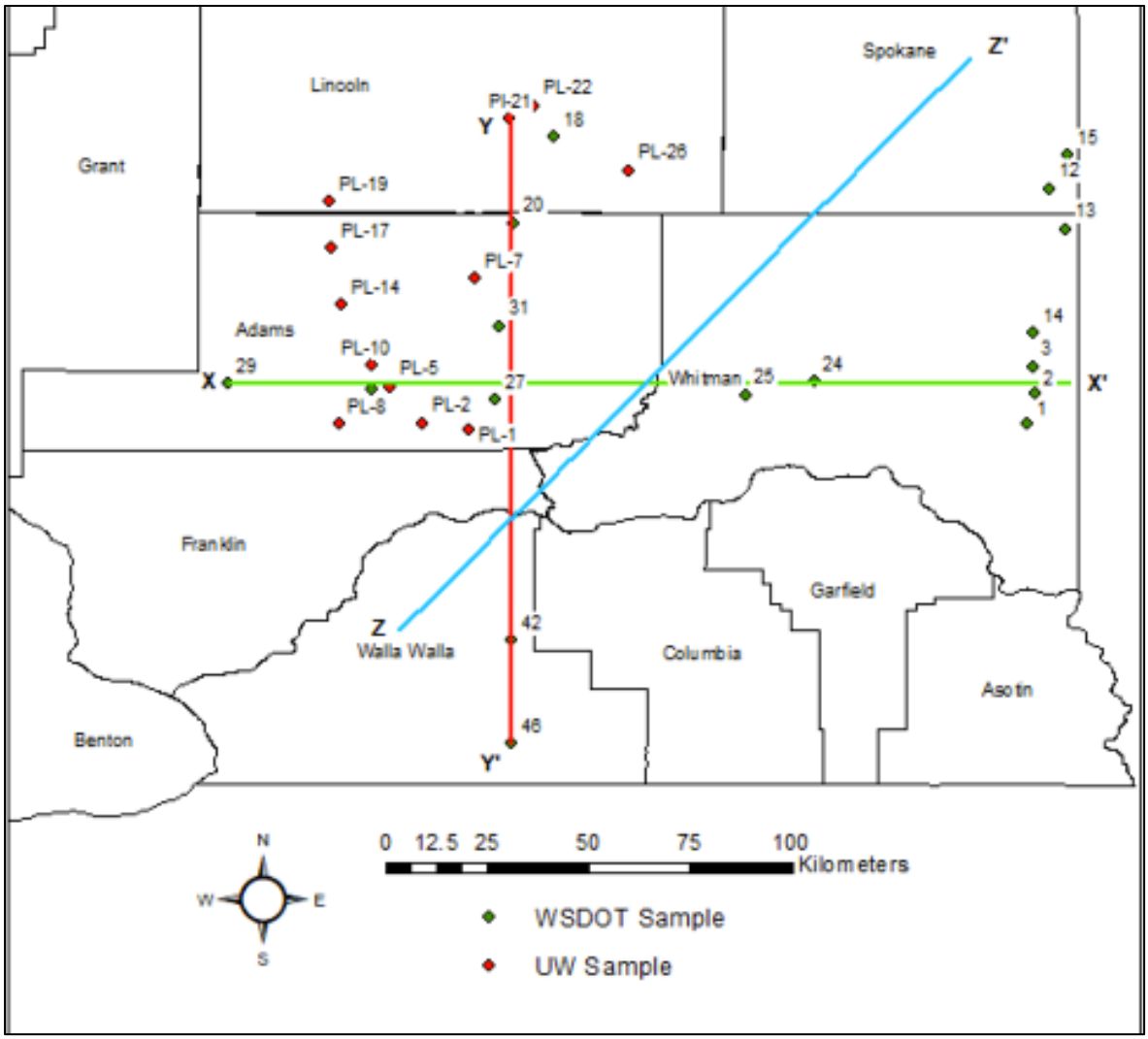

Figure 9A. Locations of transects (X to X', Y to Y', and Z to Z') and sample locations used to create each transect. Transect Z follows the purported wind direction in blue, Transect X follows East to West in green, and Transect Y follows North to South in red.

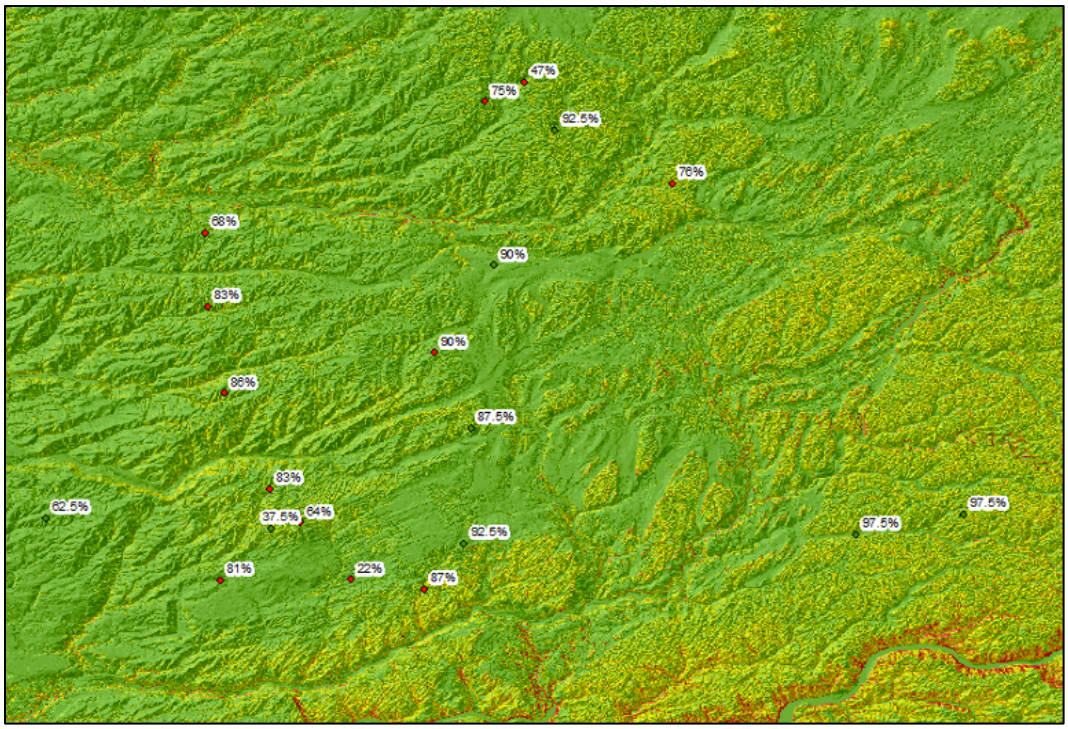

Figure 9B. Slope and Lidar used to distinguish geomorphic settings. Valley slopes are typically larger higher order streams while gulley slopes are first order or low order streams connecting to larger ones. Flats are areas of relatively little to no slope change.

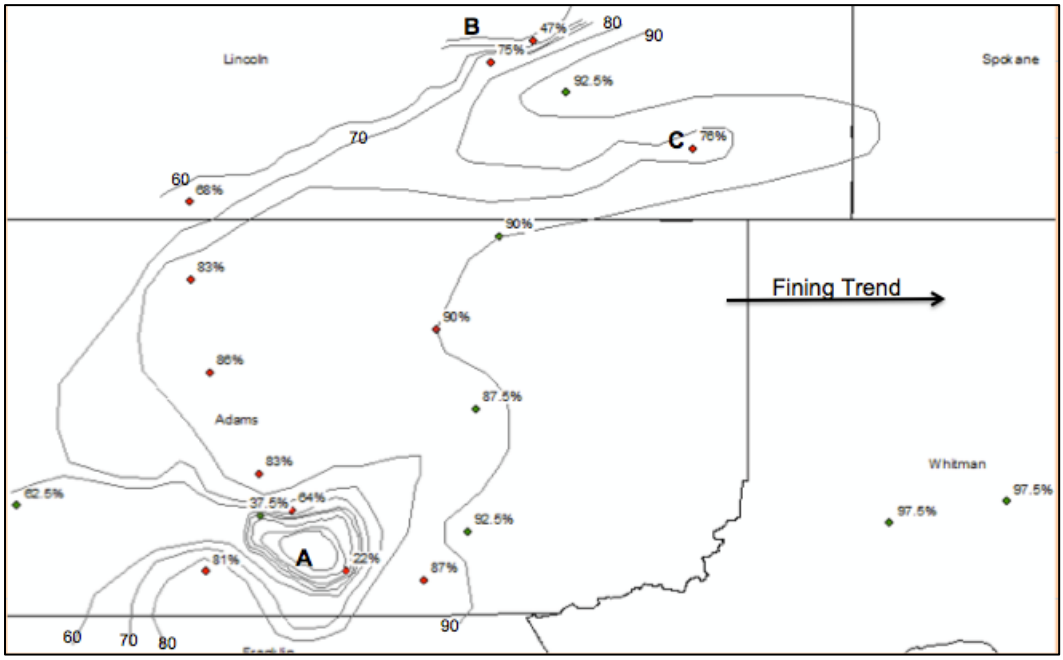

Figure 9C. Contours of percent passing when tracing similar percent passing in intervals of 10 percent.

5. Discussion

Even though our study areas were at different scales, my results are generally consistent with findings by previous researchers (Higgins et al., 1985 , McDonald et al., 2012). Higgins et al. (2012) covered broader a region and found more clayey samples. I mainly have silty to sandy loess as described in Higgins et al. 1985. The trends in my data indicate that samples from the east will plot more in the clay zone and can be distinguished from samples plotted farther west revealing the paleowind influence.

My sieve tests also show a similar pattern of slightly fining to the northeast which implies the paleowind influence but the trends are weak. After contouring my percent passing from these tests in GIS, I believe the reason for this is the presence of anomalies created by geomorphology. Anomalously low samples seem to be close in proximity to river valley channels.

A few limitations apply to this study. The sampling locations I used from Higgins et al. (1985) and transferred into ArcMap are only approximately located based on their small scale maps. The 10-meter DEM used for geomorphology is not perfectly accurate. I assumed I was sampling L1 loess based on depth information from McDonald and Busacca (1992). Depths and locations were difficult to compare between the field and their sites due to plant growth and weathering.

Surprisingly, despite apparent patterns to the naked eye, the r squared values were not as high as I anticipated when I plotted percent passing against distance in the north and south directions (Figure 10A, Figure 10C). On the other hand, r squared values for east

west trends are consistent at around 0.40 for both the WSDOT data and my data. I believe this represents a significant pattern from paleowind influence and implies the east west component of paleowind is stronger than the north south component (Figure 10A, Figure 10B, Figure 10C). The r squared values when plotting Liquid Limit against distances behaved in the opposite way with north and south being higher than east and west (Figure 11A, Figure 11B, Figure 11C). In clay percentage, the r squared is highest at around 0.675 for the east west direction(Figure 12A, Figure 12B, Figure 12C). An important distinction to make here is that the r squared mainly measures the appropriateness of a linear regression model, not necessarily the quality of the data and results.

The contours imply that tributaries and river valleys add complexity to the grain size distribution pattern (Figure 9C).

6. Conclusions

Focusing on Adams and Lincoln counties, I studied the index properties of eastern Washington loess to see if the northwest paleowind influence could be detected. After running sieve tests and Atterberg limit tests, I found definite trends in my data. Plasticity increases and Grain Size decreases downwind to the east. This means that the paleowinds are in fact detectable while studying the grain size and index properties of the loess. This confirms the inference of past researchers and can be used to make predictions about loess characteristics in localized areas in future projects. The data could be used on a county scale to predict grain size and plasticity as long as anomalies from geomorphology are accounted for. This would apply less to rivers and upland areas.

7. Recommendations

For future research, I recommend using a hydrometer analyses or laser particle size analyzer to obtain clay percentage data for my samples. These data could then be compared to the samples from Higgins et al. (1985). Obtaining these values was originally part of this study. Unfortunately, the University of Washington lab machines used to obtain the fines data were out of service due to maintenance issues during the time of this work. Other further work would include taking samples further East in Whitman County and further South in Walla Walla County. Adding data from those samples can help further calibrate the plasticity chart and percent passing graphs to better classify the loess soil types. More grain size tests can add to the amount of percent passing data available to increase accuracy. A kriging interpolation process in GIS can help with creating a better model to understand the anamolies or wind influence and would be appropriate to precisely evaluate my spatial correlated distances and directional bias.

References

Busacca, A. J. ,1991, Loess deposits and soils of the Palouse and vicinity, *in* Baker, V.R., Bjornstad, B.N., Busacca, A.J., Fecht, K.R., Kiver, E.P., Moody, U.L. Rigby, J.G., Stradling, D.F. and Tallman, A.M., The Columbia Plateau, Ch. 8 *in* Morrison, R.B. ed., Quaternary Non-Glacial Geology of the United States: Boulder, Colorado, Geological Society of America, Geology of North America, v. K-2, p. 216-228

Busacca, A. J., and McDonald, E.V., 1994, Regional sedimentation of late Quaternary loess on the Columbia Plateau: Sediment source areas and loess distribution patterns: Washington Division of Geology and Earth Resources Bulletin, v. 80, p. 181-190.

Foley, L.L., 1982, Quaternary chronology of the Palouse loess near Washtucna, WA, M.S. Thesis, Western Washington University, Bellingham, WA, 137 p.

Gaylord, D.R., Sweeney, M., Foit, F.F., Jr., McDonald, E.V., and Roberts, H.M., 2014, Overview of the geomorphic, sedimentary, stratigraphic, and paleoclimate history of sand-dominated Quaternary eolian deposits on the Columbia Plateau, WA: Geological Society of America Abstracts with Programs, v. 46, no. 6, p. 591

Gaylord, D. R., Busacca, A. J., & Sweeney, M. R. ,2003, The Palouse loess and the Channeled Scabland: a paired Ice-Age geologic system, Quaternary Geology of the United States, INQUA, p. 122-134.

Hanson, M. A., and Clague, J. J. , 2016, Record of glacial Lake Missoula floods in glacial Lake Columbia, Washington, Quaternary Science Reviews, 133, p. 62-76.

Higgins, Jerry D., Fragaszy, Richard K, Beard, Lawrence D., 1985. Development of Guidelines for Cuts in Loess Soils (Phase I). Washington State Transportation Center. WA-RD 06.1.

Ludwig, S.L., 1987, Sand within silt; The source and deposition of loess in eastern Washington [M.S. thesis]: Pullman, Washington State University, 120 p.

McDonald, E. V., 1987, Correlation and interpretation of the stratigraphy of the Palouse loess of eastern Washington [M.S. thesis]: Pullman, Washington, Washington State University, p. 218

McDonald, E. V., & Busacca, A. J.,1992, Late Quaternary stratigraphy of loess in the Channeled Scabland and Palouse regions of Washington State, Quaternary Research, 38(2), p. 141-156.

McDonald, E. V., Sweeney, M. R., & Busacca, A. J.,2012, Glacial outburst floods and loess sedimentation documented during Oxygen Isotope Stage 4 on the Columbia Plateau, Washington State, Quaternary Science Reviews, 45, p. 18-30.

Sweeney, M. R., Busacca, A. J., Richardson, C. A., Blinnikov, M., & McDonald, E. V. ,2004, Glacial anticyclone recorded in Palouse loess of northwestern United States, Geology, 32(8), p. 705-708.

Sweeney, M. R., Busacca, A. J., & Gaylord, D. R. , 2005, Topographic and climatic influences on accelerated loess accumulation since the last glacial maximum in the Palouse, Pacific Northwest, USA. Quaternary Research, 63(3), p. 261-273.

Sweeney, M. R., Gaylord, D. R., & Busacca, A. J. , 2007, Evolution of Eureka Flat: A dust-producing engine of the Palouse loess, USA. Quaternary International, 162, p. 76-96.

Sweeney, M. R., McDonald, E. V., & Gaylord, D. R. , 2017, Generation of the Palouse loess: Exploring the linkages between glaciation, outburst megafloods, and eolian deposition in Washington State. From the Puget Lowland to East of the Cascade Range: Geologic Excursions in the Pacific Northwest, 49, p. 207.

Appendix

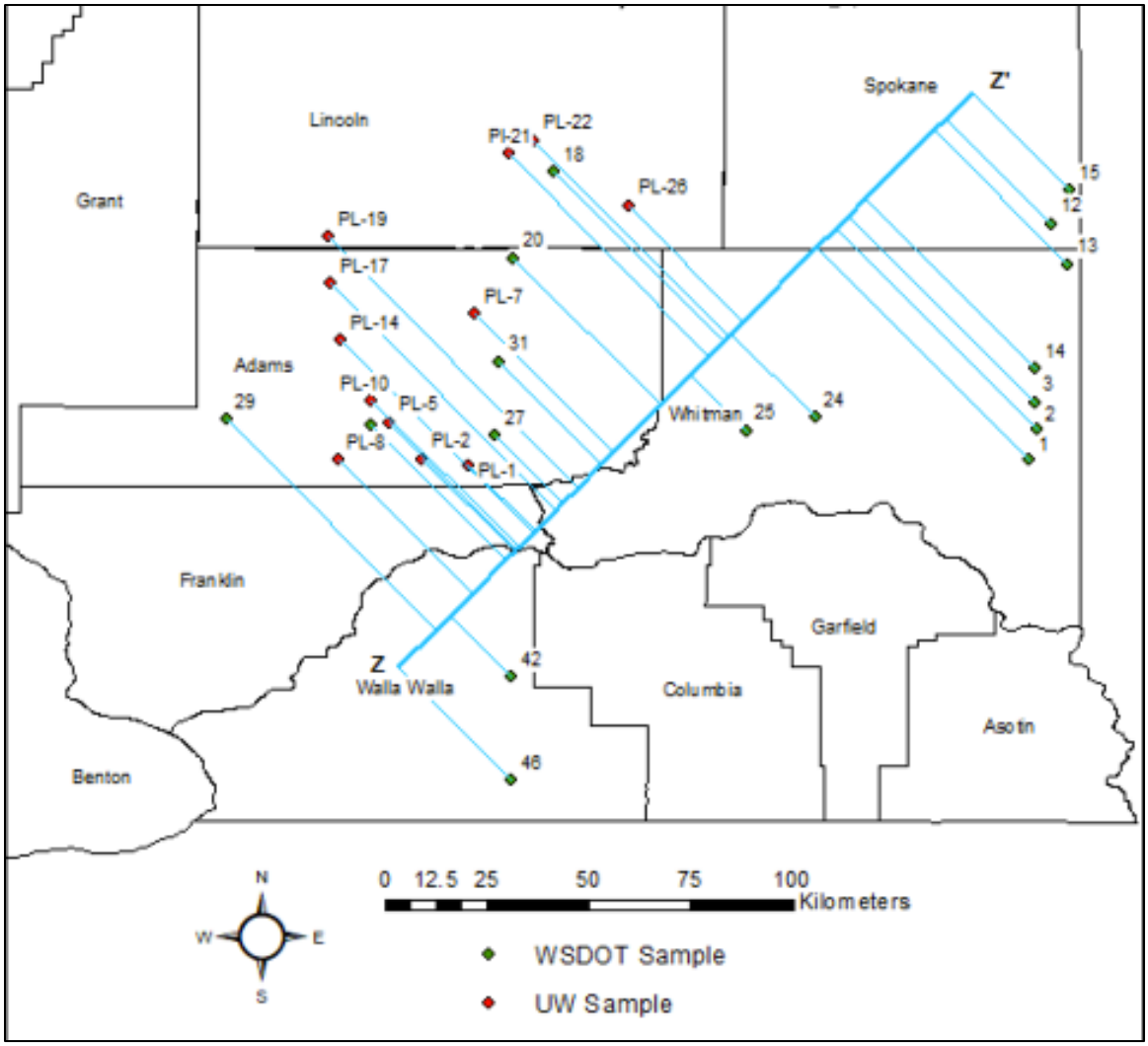

Figure 9D. Transect Z to Z' with points linked to determine distances along the transect.

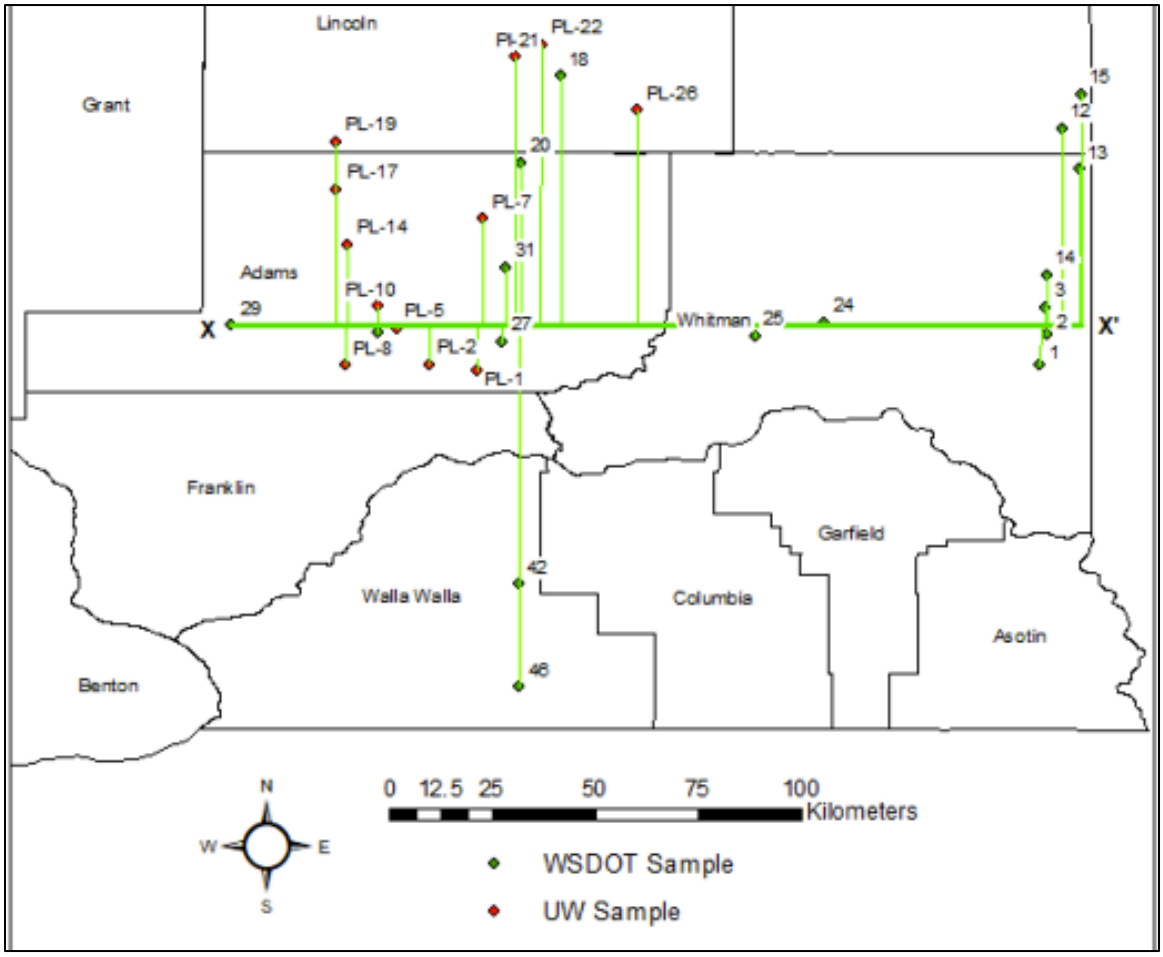

Figure 9E. Transect X to X' with points linked to determine distances along the transect.

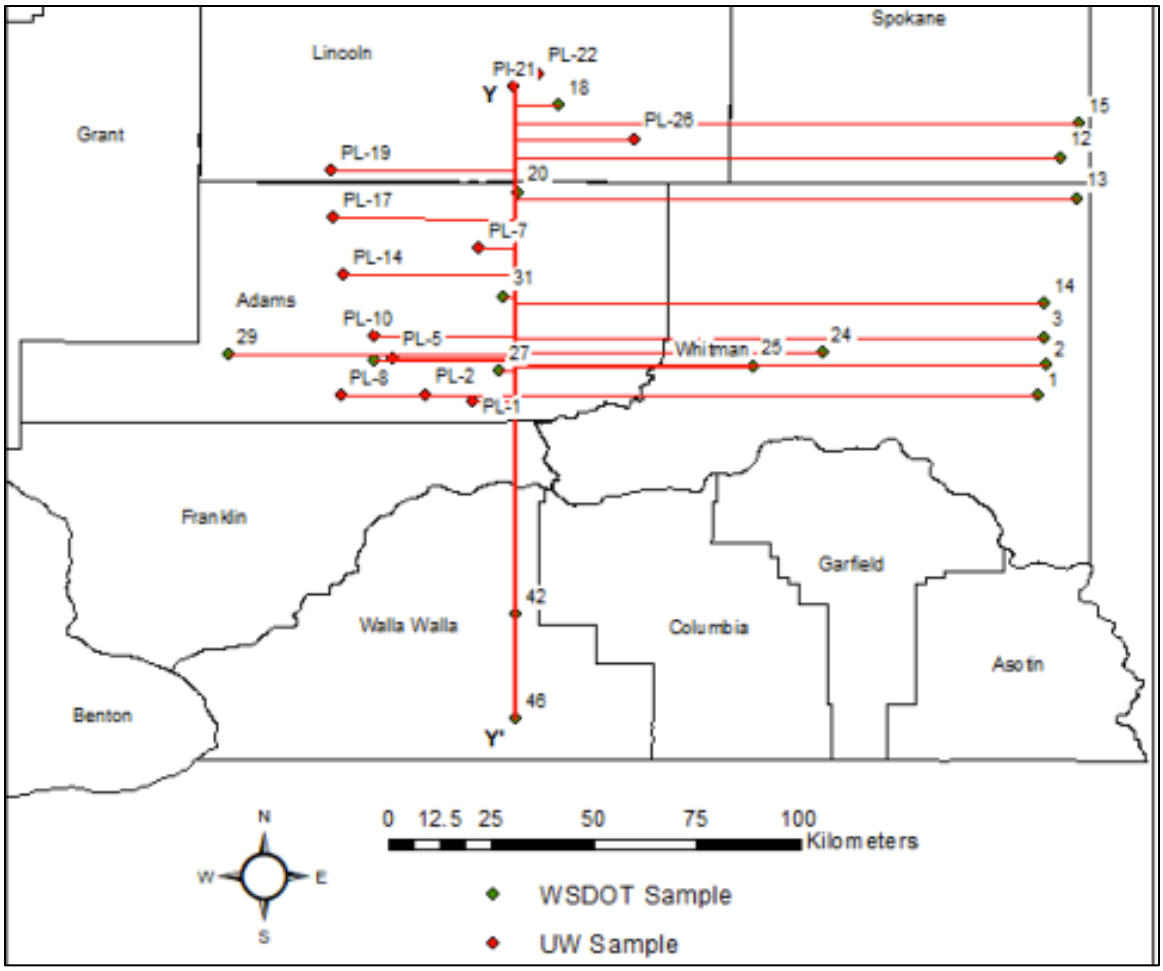

Figure 9F. Transect Y to Y' with points linked to determine distances along the transect.

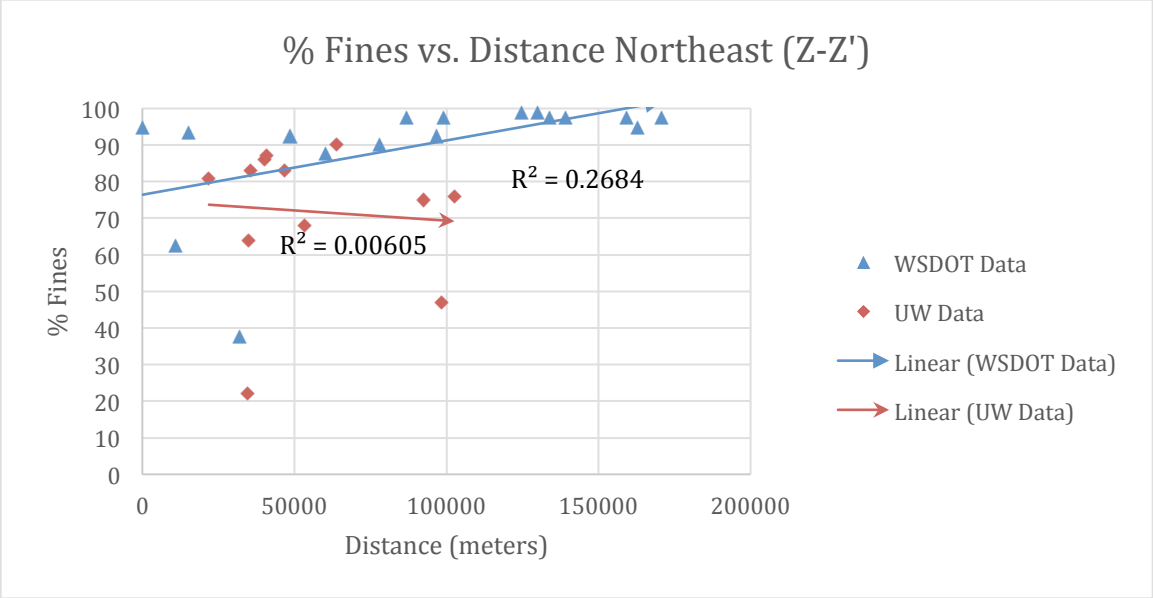

Figure 10A. The Percent passing graph of Transect Z to Z' represents the amount of fine to coarse grains in each sample with more passing representative of finer grains.

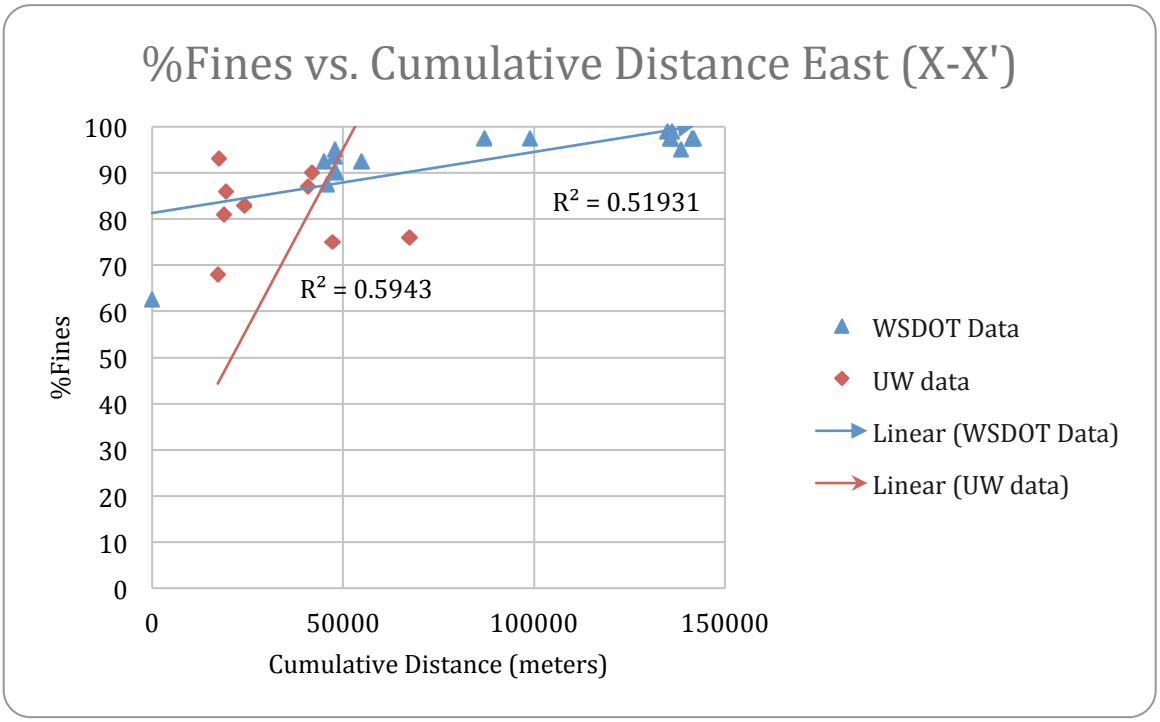

Figure 10B. Percent passing graph of Transect X to X'.

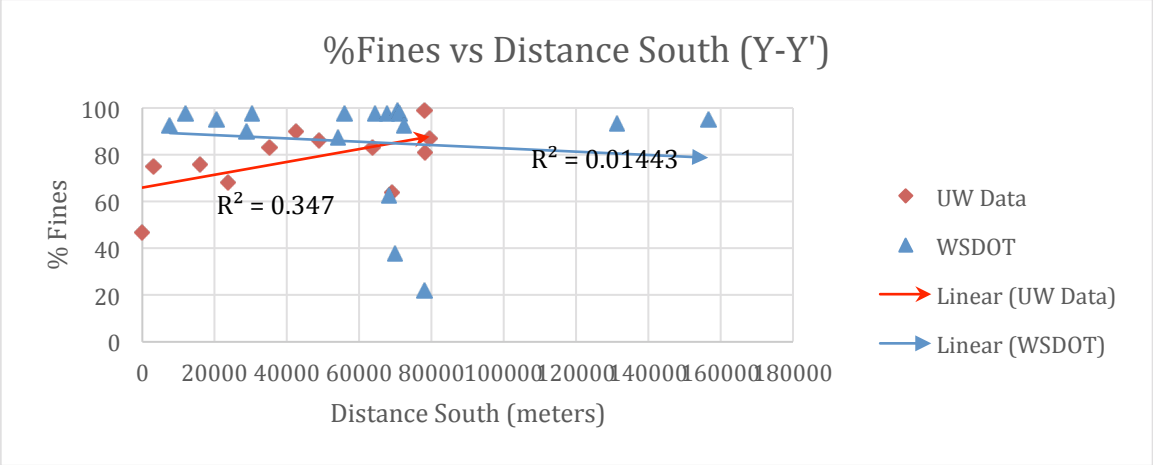

Figure 10C. Percent passing graph of Transect Y to Y'.

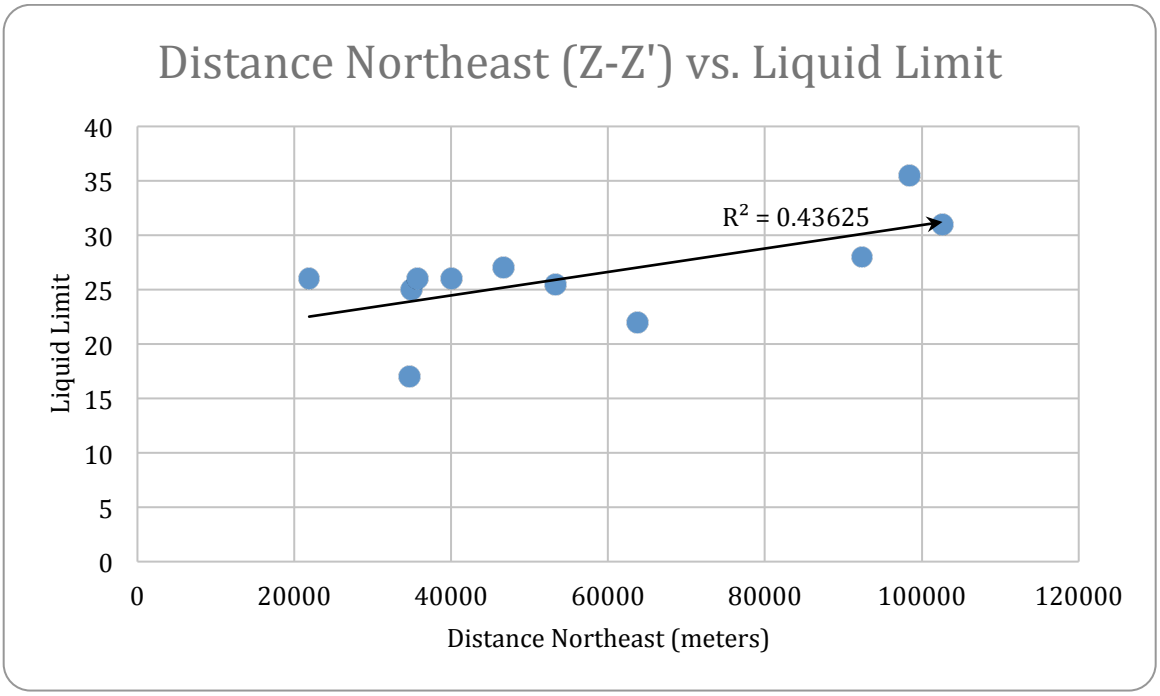

Figure 11A. Liquid Limit graph for University of Washington samples based on Transect Z to Z'.

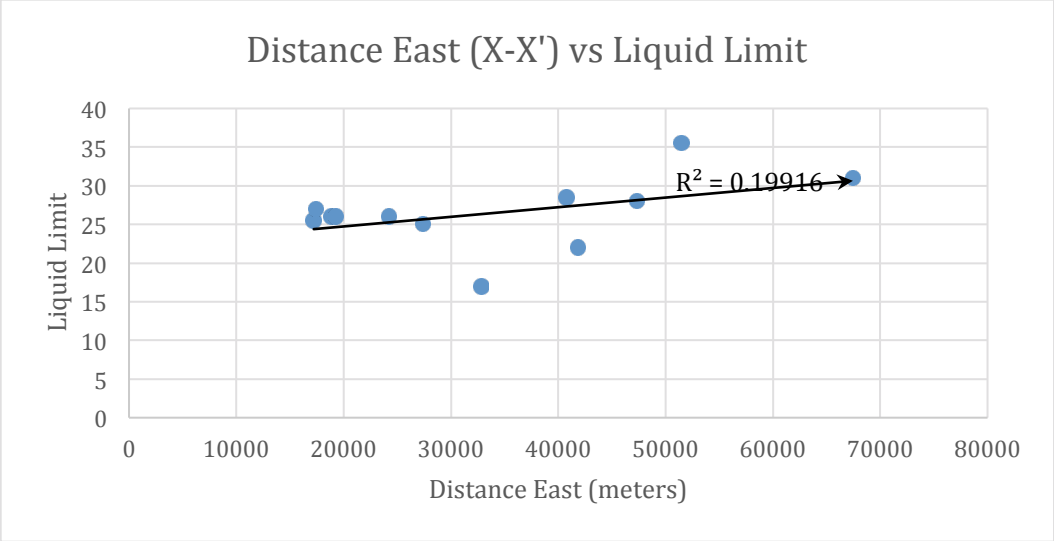

Figure 11B. Liquid Limit graph for University of Washington samples based on Transect X to X'.

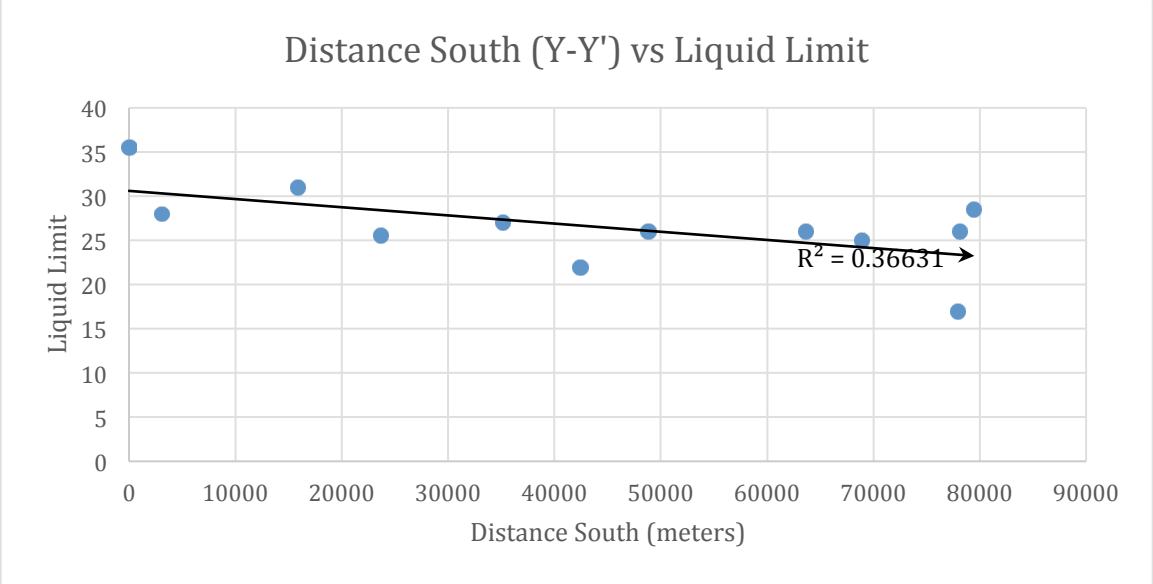

Figure 11C. Liquid Limit graph for University of Washington samples based on Transect Y to Y'.

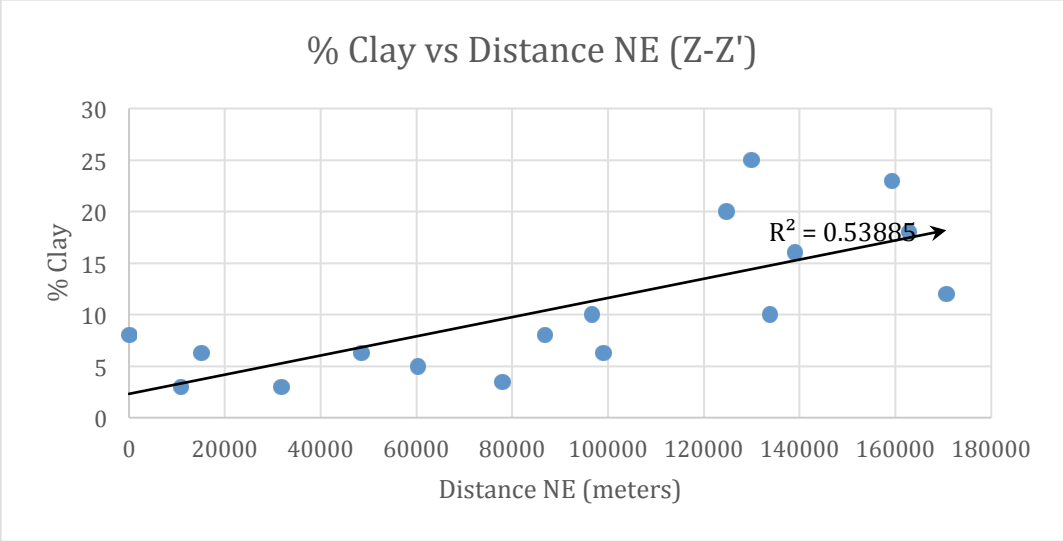

Figure 12A. Clay percentage graph for Transect Z to Z' created using sample data from Higgins et al., (1985).

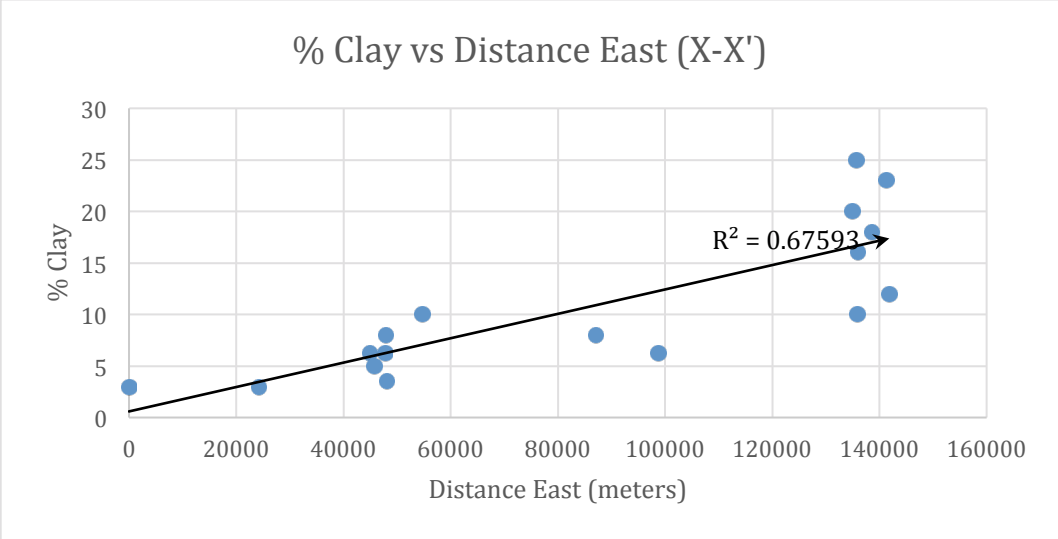

Figure 12B. Clay percentage graph for Transect X to X' created using sample data from Higgins et al., (1985).

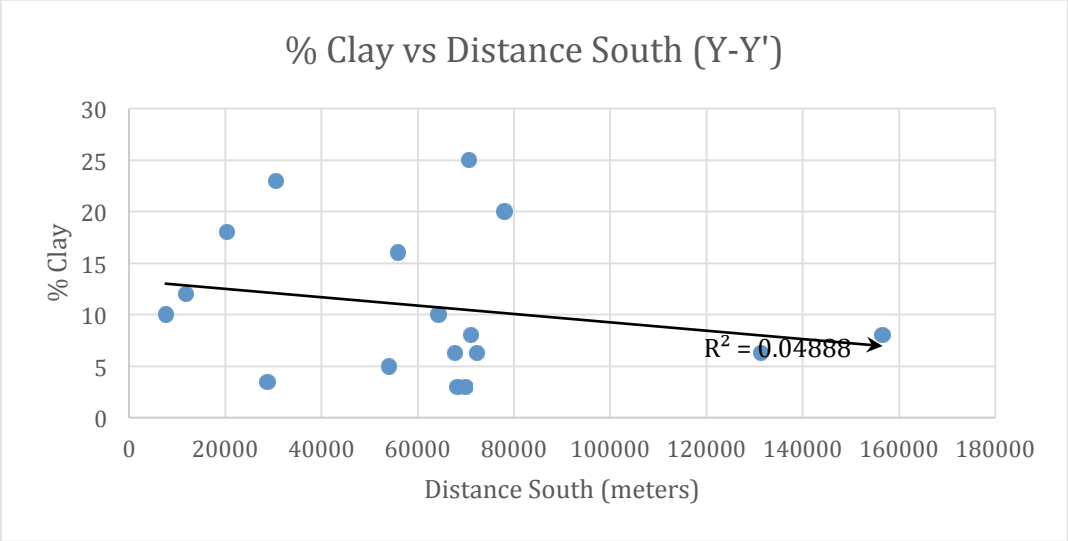

Figure 12C. Clay percentage graph for Transect Y to Y' created using sample data from Higgins et al., (1985).